

Deep Learning for MIMO Channel Estimation: Interpretation, Performance, and Comparison

Qiang Hu, Feifei Gao, *Senior Member, IEEE*, Hao Zhang, Shi Jin, *Senior Member, IEEE*, and Geoffrey Ye Li, *Fellow, IEEE*

Abstract

Deep learning (DL) has emerged as an effective tool for channel estimation in wireless communication systems, especially under some imperfect environments. However, even with such unprecedented success, DL methods still serve as black boxes and the lack of explanations on their internal mechanism severely limits further improvement and extension. In this paper, we present a preliminary theoretical analysis on DL based channel estimation for multiple-antenna systems to understand and interpret its internal mechanism. Deep neural network (DNN) with rectified linear unit (ReLU) activation function is mathematically equivalent to a set of local linear functions corresponding to different input regions. Hence, the DL estimator built on it can achieve universal approximation to a large family of functions by making efficient use of piecewise linearity. We demonstrate that DL based channel estimation does not restrict to any specific signal model and will approach to the minimum mean-squared error (MMSE) estimation in various scenarios without requiring any prior knowledge of channel statistics. Therefore, DL based channel estimation outperforms or is comparable with traditional channel estimation. Simulation results confirm the accuracy of the proposed interpretation and demonstrate the effectiveness of DL based channel estimation under both linear and nonlinear signal models.

Index Terms

Explainable deep learning, input space partition, channel estimation, MIMO, ReLU.

Q. Hu and H. Zhang are with the Department of Electrical Engineering, Tsinghua University, Beijing 100084, P. R. China (e-mail: huq16@mails.tsinghua.edu.cn; haozhang@mail.tsinghua.edu.cn).

F. Gao is with the Institute for Artificial Intelligence, Tsinghua University (THUAI), State Key Lab of Intelligent Technologies and Systems, Tsinghua University, Beijing National Research Center for Information Science and Technology (BNRist), Department of Automation, Tsinghua University, Beijing 100084, P. R. China (e-mail: feifeigao@ieee.org).

S. Jin is with the National Mobile Communications Research Laboratory, Southeast University, Nanjing 210096, P. R. China (e-mail: jinshi@seu.edu.cn).

G. Y. Li is with the School of Electrical and Computer Engineering, Georgia Institute of Technology, Atlanta, GA, USA (e-mail: liye@ece.gatech.edu).

I. INTRODUCTION

Deep learning (DL) in wireless communications are making profound technological revolution to its concepts, patterns, methods and means [1]–[3]. Currently, most research focuses on enhancing functionalities at the physical layer (PHY) [4] or network level of communication systems [5], [6], including channel estimation [7], [8], channel state information (CSI) feedback compression [9], signal detection [10], and resource management [11], etc. Among all DL applications to wireless communication systems, channel estimation is one of the most widely studied issues. The authors in [8] have made the first attempt to apply powerful DL methods to learn the characteristics of frequency selective wireless channels and combat the nonlinear distortion and interference for orthogonal frequency division multiplexing (OFDM) systems. The authors in [12] have developed a novel framework that incorporates DL methods into massive multiple-input multiple-output (MIMO) systems in a bid to address direction-of-arrival (DoA) estimation and channel estimation problems. In [13], DL based channel estimation is extended to doubly selective channels and has numerically demonstrated better performance than conventional estimators in many scenarios. In [14], the channel matrix is regarded as an image and DL based image super-resolution and denoising techniques are employed to estimate the channel. Furthermore, a sparse complex-valued neural network structure is proposed in [15] to tackle channel estimation in massive MIMO systems. Another branch of research attempts to establish novel, end-to-end deep neural networks (DNN) architecture to replace all modules at the transmitter and at the receiver, respectively, in a communication system [16], [17].

The above works have achieved great success across a variety of tasks over the recent years. Despite the rapid development of DL, the DNN embedded wireless communication system is generally considered as a black box for signal transmission/reception [4]. Only numerical and experimental evaluations are available to demonstrate the powerful capability of DL in learning key functional components of wireless systems are available, and there is nearly no analytical support to confirm the advantages of DL methods when applied to communications. Clearly, interpreting how and why DL methods achieve astounding performance for a wide range of tasks is desired for further performance improvement and extension to different environments.

Another important issue is to figure out how well the performance of newly emerged data-driven DL methods is compared to traditional expert-designed algorithms in the field of wireless communications [18]. Phenomena in PHY communications, such as noise, channel fading, interference, etc, have been thoroughly understood and addressed by well-established signal and coding theories from both practical and theoretical perspectives. It is yet unclear whether the black-box DL methods, originally designed for

structured tasks that can be easily handled by human while hardly solved by analytical methods, would be able to outperform the existing white-box approaches. In addition, the regular ways of signal processing have been overturned by DL methods, in which satisfactory performance is still attainable in the absence of expert knowledge that is vital for conventional methods. Whether DL methods for communications are trustful or not when employed to communication systems is unknown yet and needs further exploration. The unsolved issues drive us to investigate and explain DL methods.

There have been a rich history addressing the complicated inner-workings of DL methods. The very first results have demonstrated a universal approximation of DNNs that any continuous function defined on compact sets can be approximated at any precision using DNNs [19], [20]. Recently, some effort has been made to analyze how the structural properties of DNNs, mainly depth and width, contribute to their powerful capability of modeling functions, i.e., expressiveness of DNNs [21]–[23]. These works converge to a similar conclusion that the expressive power of a DNN grows exponentially with its depth, which is compelling and provides some meaningful theoretical insights into superior performance of DNNs in practice.

Though more and more research has evidenced that DL methods are particularly suited to channel estimation, an analytical interpretation of this phenomenon is still missing. A comprehensive understanding of DL method's behavior on estimating channels is expected to provide guidance and inspiration for the further exploitation on DL based estimation theory. In this paper, we present an initial attempt on interpreting DL for channel estimation in multiple-antenna systems. Our contributions are listed as follows:

- Based on the property that a DNN with rectified linear unit (ReLU) activation function (ReLU DNN) is mathematically equivalent to a set of local linear functions, we derive a closed-form expression for DL based channel estimation.
- We analyze and compare the performance of DL based channel estimation with the conventional methods, i.e., least-square (LS) and linear minimum mean-squared error (LMMSE) estimators. We demonstrate that the DL estimator built on ReLU DNNs is more flexible than the conventional estimation methods and can well approximate the minimum mean-squared error (MMSE) estimator under certain requirements.
- We find and prove that a DL estimator is highly sensitive to the quality of training data. Therefore, the performance of DL based channel estimation will significantly degrade compared to conventional estimation methods if the statistics of training data mismatch with deployed environments.

The rest of this paper is organized as follows. The system model and the traditional and DL based

channel estimation methods are introduced in Section II. The internal mechanisms of ReLU DNNs are described in Section III. The DL based channel estimation under linear and nonlinear systems is discussed in Section IV. The channel estimation with inaccurate training data is presented in Section V. The simulation results are provided in Section VI followed by the conclusions in Section VII.

Notations: We use lowercase letters and capital letters in boldface to denote vectors and matrices, respectively. In particular, \mathbf{I}_M denotes the $M \times M$ identity matrix. The notations $(\cdot)^T$, $(\cdot)^*$, and $(\cdot)^H$ denote the transpose, conjugate, and conjugate transpose of a matrix, respectively. $\mathbb{E}\{\cdot\}$ denotes the expectation, and $\text{tr}\{\cdot\}$ denotes the trace of a matrix. The cardinality of a set is denoted by $|\cdot|$. The notation $\|\cdot\|_2$ denotes the L_2 norm, and $\text{diag}\{\mathbf{x}\}$ denotes a diagonal matrix with all elements in \mathbf{x} at the main diagonal.

II. SYSTEM MODEL AND CHANNEL ESTIMATION

In this section, we firstly introduce the system model for channel estimation and then present the conventional channel estimation methods and the DL based method using multiple-antenna communication as an example.

A. System Model

Consider a multiple-antenna communication system with t_0 antennas at the base station (BS) and a single antenna at the user side. Assume the uplink channel is with block fading, where channel fading is fixed within a block but varies from one to another. The traditional way of estimating channels at the BS is to use uplink pilot. Let τ be the transmitted pilot symbol with $|\tau|^2 = 1$. The received symbol at the BS can be represented by the following $t_0 \times 1$ vector

$$\mathbf{x}_0 = \tau \mathbf{h} + \mathbf{n}, \quad (1)$$

where \mathbf{h} denotes the $t_0 \times 1$ random channel vector between the BS and the user and \mathbf{n} is the $t_0 \times 1$ white noise vector with zero-mean and element-wise variance σ_n^2 . We assume that the channel vector \mathbf{h} is zero mean and with covariance matrix $\mathbf{R} = \mathbb{E}\{\mathbf{h}\mathbf{h}^T\}$ ¹.

B. Conventional Channel Estimation

The goal of channel estimation is to extract \mathbf{h} from \mathbf{x}_0 as accurate as possible. The conventional estimation methods are based on the expert knowledge and the signal model in (1).

¹In general, the complex valued signals would decompose into real values before inputting to ReLU DNNs. For convenience, we assume that both of input signals and channels are real values.

1) *LS Channel Estimator*: From (1), we derive the LS estimate of \mathbf{h} as [24]

$$\hat{\mathbf{h}}_{\text{LS}} = \frac{1}{\tau} \mathbf{x}_0 = \mathbf{h} + \frac{1}{\tau} \mathbf{n}, \quad (2)$$

and the corresponding MSE is

$$J_{\text{LS}} = \mathbb{E}\{\|\mathbf{h} - \hat{\mathbf{h}}_{\text{LS}}\|^2\} = \sigma_n^2 t_0. \quad (3)$$

As shown in (3), the performance of the LS estimator is inversely proportional to the signal-to-noise ratio (SNR) defined as $1/\sigma_n^2$. Since the LS estimator requires no prior knowledge of channel statistics, it is easy to implement.

2) *LMMSE Channel Estimator*: The general form of LMMSE estimator exploits the signal model in (1) and channel statistics. It can be expressed as [24]

$$\hat{\mathbf{h}}_{\text{LMMSE}} = \mathbf{R} (\mathbf{R} + \sigma_n^2 \mathbf{I}_{t_0})^{-1} \mathbf{x}_0. \quad (4)$$

Then, the MSE of the LMMSE estimator is computed as

$$J_{\text{LMMSE}} = \text{tr}\left\{\mathbf{R} \left(\mathbf{I}_{t_0} + \frac{1}{\sigma_n^2} \mathbf{R}\right)^{-1}\right\} \leq J_{\text{LS}}, \quad (5)$$

which is always smaller than that of the LS estimator.

The LMMSE channel estimation leads to a more accurate estimate by utilizing the second order statistics of channels, and therefore the performance of the LMMSE estimator is sensitive to the imperfection of channel statistics. However, this information is difficult to perfectly acquire in practice. On the contrary, the LS estimator can be readily deployed in various scenarios due to its simplicity, but its accuracy is relatively low compared to the LMMSE estimator. Recently, the DL estimator has emerged as a promising alternative to address channel estimation in wireless communication systems. The strong robustness and excellent learning capacity of the DL estimator make it a powerful tool for channel estimation in imperfect and interference corrupted systems.

C. DL based Channel Estimation

Consider a DL estimator \mathcal{P} with a K -layer fully-connected ReLU DNN, as illustrated in Fig. 1. The input and output of \mathcal{P} are denoted by $\mathbf{x}_0 \in \mathcal{X} \subseteq \mathbb{R}^{t_0}$ and $\mathbf{h} \in \mathcal{H} \subseteq \mathbb{R}^{t_0}$, respectively, where \mathcal{X} and \mathcal{H} are the input space and the output space. Let $g(\mathbf{x}_0, \theta)$ be the $\mathbb{R}^{t_0} \rightarrow \mathbb{R}^{t_0}$ function that \mathcal{P} represents, where θ denotes all the parameters of \mathcal{P} , and $g(\mathbf{x}_0, \theta)$ is the estimated channel of the DL estimator. Let $\mathcal{Z} = \mathcal{X} \times \mathcal{H}$ be the sample space of training. A set of training samples drawn from the joint distribution of \mathbf{x}_0 and \mathbf{h} is denoted by $Z_m = \{z_i\}_{i=1}^m = \{(\mathbf{x}_{0,i}, \mathbf{h}_i)\}_{i=1}^m$, where m is the number of training samples.

where $\mathbf{W}_o \in \mathbb{R}^{t_o \times t_K}$ and $\mathbf{b}_o \in \mathbb{R}^{t_o}$ are the weight matrix and the bias vector of the output layer, respectively.

III. INTERNAL MECHANISM OF ReLU DNNs

In this section, a detailed description on the learning mechanism of ReLU DNNs for DL based channel estimation is provided. We show that ReLU DNNs are in fact piecewise linear (PWL) functions with their input space partitioned into a set of linear regions according to different activation patterns of neurons. The DL estimators powered by ReLU DNNs are very flexible and can model a rich set of functions.

A. Input Space Partition

As discussed in [25], the input space of a ReLU DNN is partitioned into different regions according to the corresponding activation patterns so that the DNN turns into a linear mapping in each region. Since ReLU function is PWL, the neurons in \mathcal{P} consist of only two states: with zero output or replicating input. Denote by $s_{k,i} \in \{0, 1\}$ the state of neuron i of the k -th hidden layer such that $s_{k,i} = 0$ if $g_{k,i} \leq 0$ and $s_{k,i} = 1$ otherwise, where $g_{k,i}$ is the i -th element of $g_k(\mathbf{x}_{k-1})$ for $i \in \{1, \dots, t_k\}$. Define the activation pattern of all neurons at the k -th hidden layer as a vector $\mathbf{s}_k = [s_{k,1}, \dots, s_{k,t_k}]^T$. The activation pattern of \mathcal{P} can be expressed as a t -dimensional vector $\mathbf{s}_{\mathcal{P}} = [\mathbf{s}_1^T, \dots, \mathbf{s}_K^T]^T$, where $t = \sum_{k=1}^K t_k$ is the total number of hidden neurons.

From the definition, $\mathbf{s}_{\mathcal{P}}$ is determined by \mathbf{x}_0 once θ is fixed. Denote the function $\mathcal{F}(\mathbf{x}_0) : \mathcal{X} \rightarrow \mathcal{S}$ as the mapping from the input space \mathcal{X} to the space of activation patterns \mathcal{S} , where $\mathcal{S} \subseteq \{0, 1\}^t$ denotes the set of all possible activation patterns of \mathcal{P} . Let $v = |\mathcal{S}|$ be the cardinality of \mathcal{S} . Given an activation pattern $\mathbf{s}_{\mathcal{P},i} \in \mathcal{S}$, only certain inputs over \mathcal{X} correspond to $\mathbf{s}_{\mathcal{P},i}$, and the input space is then partitioned into a set of v disjoint regions based on the activation patterns. Denote $\mathcal{X}_i = \{\mathbf{x}_0 \in \mathcal{X} \mid \mathcal{F}(\mathbf{x}_0) = \mathbf{s}_{\mathcal{P},i} \forall \mathbf{s}_{\mathcal{P},i} \in \mathcal{S}\}$ as the input region with the same activation pattern. From the above discussion, there are

$$\begin{aligned} \mathcal{X}_i &\subseteq \mathcal{X}, \quad i = 1, \dots, v, \\ \mathcal{X} &= \cup_{i=1}^v \mathcal{X}_i, \\ \mathcal{X}_i \cap \mathcal{X}_{i'} &= \emptyset, \quad \forall i \neq i'. \end{aligned} \tag{10}$$

For any input $\mathbf{x}_0 \in \mathcal{X}_i$ and its corresponding activation pattern $\mathbf{s}_{\mathcal{P},i}$ of \mathcal{X}_i , the pre-activation $g_{k+1}(\mathbf{x}_k)$ can be expanded as

$$\begin{aligned} g_{k+1}(\mathbf{x}_k) &= \mathbf{W}_{k+1}\mathbf{x}_k + \mathbf{b}_{k+1} = \mathbf{W}_{k+1}\mathbf{\Lambda}_k g_k(\mathbf{x}_{k-1}) + \mathbf{b}_{k+1} \\ &= \tilde{\mathbf{W}}_{k+1} g_k(\mathbf{x}_{k-1}) + \mathbf{b}_{k+1}, \end{aligned} \tag{11}$$

where $\tilde{\mathbf{W}}_{k+1} = \mathbf{W}_{k+1}\mathbf{\Lambda}_k$ and $\mathbf{\Lambda}_k = \text{diag}\{\mathbf{s}_k\}$, respectively. Note that there is $\tilde{\mathbf{W}}_1 = \mathbf{W}_1$ at the first hidden layer. By recursively expanding $g_{k+1}(\mathbf{x}_k)$ layer by layer, we can further express $g_{k+1}(\mathbf{x}_k)$ as

$$\begin{aligned} g_{k+1}(\mathbf{x}_k) &= \prod_{i=1}^{k+1} \tilde{\mathbf{W}}_i \mathbf{x}_0 + \sum_{i=1}^k \left(\prod_{j=1}^i \tilde{\mathbf{W}}_{i+1-j} \right) \mathbf{b}_{i+1-j} + \mathbf{b}_k \\ &= \hat{\mathbf{W}}_{k+1} \mathbf{x}_0 + \hat{\mathbf{b}}_{k+1}, \end{aligned} \quad (12)$$

where $\hat{\mathbf{W}}_{k+1} = \prod_{i=1}^{k+1} \tilde{\mathbf{W}}_i$ is the equivalent weight matrix with respect to (w.r.t) the input \mathbf{x}_0 , and the sum of the remaining terms is denoted by $\hat{\mathbf{b}}_k = \sum_{i=1}^{k-1} \left(\prod_{j=1}^i \tilde{\mathbf{W}}_{i+1-j} \right) \mathbf{b}_{i+1-j} + \mathbf{b}_k$. Substituting (12) into (9), we obtain the explicit form of $g(\mathbf{x}_0, \theta)$ for $\mathbf{x}_0 \in \mathcal{X}_i$ as

$$g_{\mathcal{X}_i}(\mathbf{x}_0) = \mathbf{W}_{\mathcal{X}_i} \mathbf{x}_0 + \mathbf{b}_{\mathcal{X}_i}, \quad (13)$$

where $\mathbf{W}_{\mathcal{X}_i} = \mathbf{W}_o \mathbf{\Lambda}_K \hat{\mathbf{W}}_K$ and $\mathbf{b}_{\mathcal{X}_i} = \mathbf{W}_o \mathbf{\Lambda}_K \hat{\mathbf{b}}_K + \mathbf{b}_o$.

Since both $\mathbf{W}_{\mathcal{X}_i}$ and $\mathbf{b}_{\mathcal{X}_i}$ are determined by \mathcal{X}_i , $g_{\mathcal{X}_i}(\mathbf{x}_0)$ in (13) is uniquely determined by \mathcal{X}_i . All the inputs, $\mathbf{x}_0 \in \mathcal{X}_i$, have the same $g_{\mathcal{X}_i}(\mathbf{x}_0)$ in (13), i.e., the same activation pattern. The boundary of these inputs dividing \mathcal{X}_i is a set of hyperplanes in \mathcal{X} since $g_{\mathcal{X}_i}(\mathbf{x}_0)$ is a local linear function [25]. Therefore, the partitioned regions $\{\mathcal{X}_1, \dots, \mathcal{X}_v\}$ are linear regions in \mathcal{X} , and $g(\mathbf{x}_0, \theta)$ is a set of $t_0 \mathbb{R}^{t_0} \rightarrow \mathbb{R}$ PWL functions over \mathcal{X} . The input region partition according to the activation pattern in [25] is a critical step to interpret DL based channel estimation and will be used in the later analysis.

B. Universal Approximation of DL Estimator

The DL estimator is particularly effective in channel estimation problems, where the explicit signal model is actually unknown, e.g., imperfect power amplifier (PA) [26], [27] and quantization error of analog to digital converter (ADC) [28]. Although the structural design and applications of the DL estimator have been extensively explored, there exists limit research to address its powerful expressiveness on function representation, i.e., the ability to model functions.

In fact, the DL estimator powered by a ReLU DNN is a universal approximator for channel estimation. From Section III-A, the function represented by the DL estimator is a set of $t_0 \mathbb{R}^{t_0} \rightarrow \mathbb{R}$ PWL functions as shown in (13). From Theorem 2.1 in [29], the reverse is also true that any $\mathbb{R}^{t_0} \rightarrow \mathbb{R}$ PWL function can be represented by a DL estimator if the underlying network satisfies certain structural requirements.

Theorem 2.1 in [29] verifies the powerful expressiveness of the DL estimator when the network depth is sufficiently large. Another well-known fact is that the PWL functions are dense in any $\mathcal{L}^q(\mathbb{R}^{t_0})$ space and can approximate any compactly supported continuous functions with arbitrary precision. Note that $\mathcal{L}^q(\mathbb{R}^{t_0})$ is the space of Lebesgue integrable functions f , where μ is the Lebesgue measure on \mathbb{R}^{t_0} and

$\int |f|^q d\mu < \infty$. Combining these two properties, the DL estimator is a universal approximator as described by the Theorem 2.3 in [29].

Theorem 2.3 in [29] shows that every function in $\mathcal{L}^q(\mathbb{R}^{t_0})$ ($1 \leq q \leq \infty$) can be arbitrarily well-approximated in the \mathcal{L}^q norm by a ReLU DNN with at most $\lceil \log_2(t_0 + 1) \rceil + 1$ layers. Hence, the DL estimator is very general and powerful. If no specific models are known a priori or complicated nonlinear systems are presented, then the DL estimator will be a preferred choice for channel estimation.

IV. ANALYSIS ON DL BASED CHANNEL ESTIMATION

Though the DL based channel estimation has shown excellent performance in various communication systems, it has seldom been analyzed from a theoretical perspective. In this section, we derive the explicit expression for DL based channel estimation with the help of the internal mechanisms of ReLU DNNs in Section III. Moreover, the LS and LMMSE estimators in Section II serve as the benchmarks to assess the estimation performance of the DL estimator.

A. Closed-form Expression for DL Channel Estimator

Different from the LS and LMMSE estimators, the DL estimator learns a set of training data Z_m drawn from certain statistical model. For the DL estimator, a non-negative loss function $\xi(g(\mathbf{x}_0, \theta), \mathbf{h})$ is needed to measure the difference between the estimated channel $g(\mathbf{x}_0, \theta)$ and the true one \mathbf{h} . We adopt the squared error as loss functions, defined as

$$J_{emp} = \frac{1}{m} \sum_{z_i \in Z_m} \xi(g(\mathbf{x}_{0,i}, \theta), \mathbf{h}_i) = \frac{1}{m} \sum_{z_i \in Z_m} \|\mathbf{h}_i - g(\mathbf{x}_{0,i}, \theta)\|_2^2, \quad (14)$$

for the empirical loss and

$$J_{DL} = \mathbb{E}_z \{ \xi(g(\mathbf{x}_0, \theta), \mathbf{h}) \} = \sum_{i=1}^v \mathbb{E} \{ \|\mathbf{h} - g(\mathbf{x}_0, \theta)\|_2^2 | \mathbf{x}_0 \in \mathcal{X}_i \} \psi(\mathcal{X}_i), \quad (15)$$

for the expected loss, where $\psi(\mathcal{X}_i)$ is the probability that \mathbf{x}_0 falls into \mathcal{X}_i .

The DL based channel estimation can be regarded as a regression problem, where the DL estimator optimizes the parameters of \mathcal{P} by minimizing the empirical loss in (14) for given Z_m and then predicts the channels from newly received signals using the optimized DL estimator.

The input space of the DL estimator is partitioned into a set of regions as depicted in (10). Let A_i be the set of index of samples that fall into \mathcal{X}_i . Note that $(|A_1|, \dots, |A_v|)$ is an i.i.d. multinomial random variable with probability $(\psi(\mathcal{X}_1), \dots, \psi(\mathcal{X}_v))$ and the constraint $\sum_{i=1}^v |A_i| = m$. Given a received signal $\mathbf{x}_0 \in \mathcal{X}_i$, $g(\mathbf{x}_0, \theta)$ is linear in \mathbf{x}_0 according to (13), and the general form of the DL estimator is simply written as

$$\hat{\mathbf{h}}_{DL,i} = \mathbf{W}_{\mathcal{X}_i} \mathbf{x}_0 + \mathbf{b}_{\mathcal{X}_i} \quad \forall \mathbf{x}_0 \in \mathcal{X}_i. \quad (16)$$

Using (16), we rewrite the empirical loss and the expected loss as

$$J_{emp} = \frac{1}{m} \sum_{i=1}^v \sum_{j \in A_i} \text{tr}\{(\mathbf{h}_j - \mathbf{W}_{\mathcal{X}_i} \mathbf{x}_{0,j} - \mathbf{b}_{\mathcal{X}_i})(\mathbf{h}_j - \mathbf{W}_{\mathcal{X}_i} \mathbf{x}_{0,j} - \mathbf{b}_{\mathcal{X}_i})^T\}, \quad (17)$$

and

$$J_{DL} = \sum_{i=1}^v \mathbb{E}[\text{tr}\{(\mathbf{h} - \mathbf{W}_{\mathcal{X}_i} \mathbf{x}_0 - \mathbf{b}_{\mathcal{X}_i})(\mathbf{h} - \mathbf{W}_{\mathcal{X}_i} \mathbf{x}_0 - \mathbf{b}_{\mathcal{X}_i})^T\} | \mathbf{x}_0 \in \mathcal{X}_i] \psi(\mathcal{X}_i), \quad (18)$$

respectively.

The optimal $\mathbf{W}_{\mathcal{X}_i}$ and $\mathbf{b}_{\mathcal{X}_i}$ are derived by minimizing the empirical loss in (17). In general, the minimization of J_{emp} requires to optimize v , $\mathbf{W}_{\mathcal{X}_i}$, and $\mathbf{b}_{\mathcal{X}_i}$ jointly while the values of $\mathbf{W}_{\mathcal{X}_i}$ and $\mathbf{b}_{\mathcal{X}_i}$ are constrained by the range they belong to. It is then very difficult to obtain an analytical optimal form of $\mathbf{W}_{\mathcal{X}_i}$ and $\mathbf{b}_{\mathcal{X}_i}$ if all these factors are taken into account. Here, we assume that $\mathbf{W}_{\mathcal{X}_i}$ and $\mathbf{b}_{\mathcal{X}_i}$ can take any values within their region. Moreover, we optimize $\mathbf{W}_{\mathcal{X}_i}$ and $\mathbf{b}_{\mathcal{X}_i}$ with v fixed firstly.

Another important issue is that only a small amount of partitioned regions within \mathcal{X} , where \mathbf{x}_0 falls into with high probabilities, contain training samples. For the regions without training samples, the DL estimator is unable to optimize its estimation and will simply output a random value. Therefore, the following optimization over $\mathbf{W}_{\mathcal{X}_i}$ and $\mathbf{b}_{\mathcal{X}_i}$ is conducted w.r.t. the regions where A_i is not empty.

Differentiating J_{emp} w.r.t. $\mathbf{b}_{\mathcal{X}_i}$, we obtain

$$\frac{\partial J_{emp}}{\partial \mathbf{b}_{\mathcal{X}_i}} = -2 \sum_{j \in A_i} (\mathbf{h}_j - \mathbf{W}_{\mathcal{X}_i} \mathbf{x}_{0,j}) + 2|A_i| \mathbf{b}_{\mathcal{X}_i}. \quad (19)$$

Setting (19) equal to zero gives

$$\mathbf{b}_{\mathcal{X}_i} = \frac{1}{|A_i|} \sum_{j \in A_i} (\mathbf{h}_j - \mathbf{W}_{\mathcal{X}_i} \mathbf{x}_{0,j}). \quad (20)$$

Substituting (20) into (17) yields the following optimization problem

$$\begin{aligned} \{\mathbf{W}_{\mathcal{X}_1}, \dots, \mathbf{W}_{\mathcal{X}_v}\} = \arg \min & \frac{1}{m} \sum_{i=1}^v \sum_{j \in A_i} [\text{tr}\{\tilde{\mathbf{h}}_j \tilde{\mathbf{h}}_j^T\} - \text{tr}\{\tilde{\mathbf{h}}_j \tilde{\mathbf{x}}_{0,j}^T \mathbf{W}_{\mathcal{X}_i}^T\} - \text{tr}\{\mathbf{W}_{\mathcal{X}_i} \tilde{\mathbf{x}}_{0,j} \tilde{\mathbf{h}}_j^T\} \\ & + \text{tr}\{\mathbf{W}_{\mathcal{X}_i} \tilde{\mathbf{x}}_{0,j} \tilde{\mathbf{x}}_{0,j}^T \mathbf{W}_{\mathcal{X}_i}^T\}], \end{aligned} \quad (21)$$

where $\tilde{\mathbf{h}}_j = \mathbf{h}_j - \frac{1}{|A_i|} \sum_{j \in A_i} \mathbf{h}_j$ and $\tilde{\mathbf{x}}_{0,j} = \mathbf{x}_{0,j} - \frac{1}{|A_i|} \sum_{j \in A_i} \mathbf{x}_{0,j}$.

Differentiating (21) w.r.t. $\mathbf{W}_{\mathcal{X}_i}$, the optimal solution to $\mathbf{W}_{\mathcal{X}_i}$ can be expressed as

$$\mathbf{W}_{\mathcal{X}_i} = \left(\sum_{j \in A_i} \tilde{\mathbf{h}}_j \tilde{\mathbf{x}}_{0,j}^T \right) \left(\sum_{j \in A_i} \tilde{\mathbf{x}}_{0,j} \tilde{\mathbf{x}}_{0,j}^T \right)^{-1}. \quad (22)$$

Plugging (22) and (20) into (16), we obtain the estimated channel when $|A_i| \neq 0$ as

$$\hat{\mathbf{h}}_{DL,i} = \left(\sum_{j \in A_i} \tilde{\mathbf{h}}_j \tilde{\mathbf{x}}_{0,j}^T \right) \left(\sum_{j \in A_i} \tilde{\mathbf{x}}_{0,j} \tilde{\mathbf{x}}_{0,j}^T \right)^{-1} \left(\mathbf{x}_0 - \frac{1}{|A_i|} \sum_{j \in A_i} \mathbf{x}_{0,j} \right) + \frac{1}{|A_i|} \sum_{j \in A_i} \mathbf{h}_j \quad \forall \mathbf{x}_0 \in \mathcal{X}_i. \quad (23)$$

Afterwards, we need to optimize $|A_i|$ in (23), whose explicit expression is difficult to calculate. Nevertheless, the explicit expression of $\hat{\mathbf{h}}_{\text{DL},i}$ in (23) remains unchanged during the optimization over $|A_i|$. Hence, we can still take $\hat{\mathbf{h}}_{\text{DL},i}$ in (23) as the optimized estimated channel of the DL estimator after training.

For a region with $|A_i| = 0$, $\mathbf{W}_{\mathcal{X}_i}$ and $\mathbf{b}_{\mathcal{X}_i}$ are randomly initialized with no explicit expressions and $\hat{\mathbf{h}}_{\text{DL},i}$ is simply given by (16).

Remark 1: To the best of our knowledge, $\hat{\mathbf{h}}_{\text{DL},i}$ in (16) or (23) is the first analytical form of the estimated channel for DL based channel estimation. From (16) and (23), the DL estimator has the simplicity and stability of linear estimator, but moves beyond the linearity by partitioning the input space into small regions. Compared to the linear estimators, e.g., the LS and LMMSE estimators, the DL estimator is more flexible and has a larger potential to combat distortion and some other unknown detrimental effects in real world communication systems.

B. Performance Assessment in Linear Systems

For linear systems, the training data, Z_m , is drawn from the linear model in (1), and the input-output pair $(\mathbf{x}_{0,i}, \mathbf{h}_i)$ can be described by

$$\mathbf{x}_{0,i} = \tau \mathbf{h}_i + \mathbf{n}_i, \quad (24)$$

for $i \in \{1, \dots, m\}$, where $\mathbf{x}_{0,i}$, \mathbf{h}_i , and \mathbf{n}_i follow the same statistical properties with \mathbf{x}_0 , \mathbf{h} , and \mathbf{n} , respectively.

Substituting (24) into (23), we can obtain the explicit expression of $\hat{\mathbf{h}}_{\text{DL},i}$. Unfortunately, the performance assessment of comparing J_{DL} and J_{LS} (J_{LMMSE}) is not straightforward since the DL estimator is highly dependent on the training samples. To reduce the impact of training samples, we focus on the case when m is sufficiently large. For the regions that $|A_i|$ is not empty, there are

$$\begin{aligned} \frac{1}{|A_i|} \sum_{j \in A_i} \mathbf{h}_j \xrightarrow{a.s.} \bar{\mathbf{h}}_i, \quad \frac{1}{|A_i|} \sum_{j \in A_i} \mathbf{x}_{0,j} \xrightarrow{a.s.} \bar{\mathbf{x}}_{0,i} \\ \frac{1}{|A_i|} \sum_{j \in A_i} \tilde{\mathbf{h}}_j \tilde{\mathbf{x}}_{0,j}^T \xrightarrow{a.s.} \mathbf{C}_{\mathbf{h}\mathbf{x}|\mathcal{X}_i}, \quad \text{and} \quad \frac{1}{|A_i|} \sum_{j \in A_i} \tilde{\mathbf{x}}_{0,j} \tilde{\mathbf{x}}_{0,j}^T \xrightarrow{a.s.} \mathbf{C}_{\mathbf{x}_0\mathbf{x}_0|\mathcal{X}_i}, \quad m \rightarrow \infty \end{aligned} \quad (25)$$

according to the law of large numbers [30], where $\xrightarrow{a.s.}$ denotes the almost sure convergence, $\bar{\mathbf{h}}_i = \mathbb{E}\{\mathbf{h}|\mathbf{x}_0 \in \mathcal{X}_i\}$, $\bar{\mathbf{x}}_{0,i} = \mathbb{E}\{\mathbf{x}_0|\mathbf{x}_0 \in \mathcal{X}_i\}$, $\mathbf{C}_{\mathbf{x}_0\mathbf{x}_0|\mathcal{X}_i}$ is the conditional covariance matrix of $\mathbf{x}_0\mathbf{x}_0^T$, and $\mathbf{C}_{\mathbf{h}\mathbf{x}_0|\mathcal{X}_i}$ is the conditional cross-covariance matrix of $\mathbf{h}\mathbf{x}_0^T$ when \mathbf{x}_0 is located at \mathcal{X}_i . According to (25), we can rewrite $\mathbf{W}_{\mathcal{X}_i}$ and $\mathbf{b}_{\mathcal{X}_i}$ as

$$\mathbf{W}_{\mathcal{X}_i} \approx \mathbf{C}_{\mathbf{h}\mathbf{x}_0|\mathcal{X}_i} \mathbf{C}_{\mathbf{x}_0\mathbf{x}_0|\mathcal{X}_i}^{-1}, \quad (26)$$

and

$$\mathbf{b}_{\mathcal{X}_i} \approx \bar{\mathbf{h}}_i - \mathbf{C}_{\mathbf{h}\mathbf{x}_0|\mathcal{X}_i} \mathbf{C}_{\mathbf{x}_0\mathbf{x}_0|\mathcal{X}_i}^{-1} \bar{\mathbf{x}}_{0i}, \quad (27)$$

respectively.

Specifically, differentiating J_{DL} w.r.t. $\mathbf{W}_{\mathcal{X}_i}$ and $\mathbf{b}_{\mathcal{X}_i}$, i.e., $\partial J_{\text{DL}}/\partial \mathbf{W}_{\mathcal{X}_i} = \mathbf{0}$ and $\partial J_{\text{DL}}/\partial \mathbf{b}_{\mathcal{X}_i} = \mathbf{0}$, we would obtain $\mathbf{W}_{\mathcal{X}_i}$ and $\mathbf{b}_{\mathcal{X}_i}$ in the same form of (26) and (27), respectively. Meanwhile, these $\mathbf{W}_{\mathcal{X}_i}$ and $\mathbf{b}_{\mathcal{X}_i}$ are exactly the weight matrix and the bias of the local LMMSE estimator for the inputs within \mathcal{X}_i . Therefore, the DL estimator derived from minimizing the empirical loss asymptotically approaches to a set of local LMMSE estimators as m gets large. Such local LMMSE estimator is the best linear estimator in \mathcal{X}_i , which, to some extent, verifies the feasibility and the effectiveness of DL estimator.

For the regions that $|A_i|$ is empty, $\mathbf{W}_{\mathcal{X}_i}$ and $\mathbf{b}_{\mathcal{X}_i}$ are random values, and the explicit forms of the corresponding J_{DL} is unable to calculate. We cannot analyze the performance of the DL estimator in this case. Nevertheless, let us consider the following inequality [31]

$$\sum_{i=1}^v \left| \frac{|A_i|}{m} - \psi(\mathcal{X}_i) \right| \leq \sqrt{\frac{2v \ln 2 + 2 \ln(1/\delta)}{m}}, \quad (28)$$

which holds with probability at least $1 - \delta$ for any $\delta > 0$. Thus, when $|A_i| \neq 0$ and m gets large, $|A_i|/m$ asymptotically approaches to $\psi(\mathcal{X}_i)$ according to (28). Moreover, $\psi(\mathcal{X}_i)$ is close to zero when $|A_i| = 0$ and m is large. Therefore, the estimated channels from the regions with empty training samples have nearly no impact on J_{DL} . For simplicity, we assume that $\mathbf{W}_{\mathcal{X}_i}$ and $\mathbf{b}_{\mathcal{X}_i}$ in these regions follow the same forms as in (26) and (27). Substituting (27) into (18) yields

$$\begin{aligned} J_{\text{DL}} &= \text{tr} \left\{ \sum_{i=1}^v \mathbb{E} [(\mathbf{h} - \hat{\mathbf{h}}_{\text{DL},i})(\mathbf{h} - \hat{\mathbf{h}}_{\text{DL},i})^T | \mathbf{x}_0 \in \mathcal{X}_i] \psi(\mathcal{X}_i) \right\} \\ &= \text{tr} \left\{ \sum_{i=1}^v \mathbb{E}_{\mathbf{x}_0 \in \mathcal{X}_i} [[(\mathbf{h} - \bar{\mathbf{h}}_i) - \mathbf{W}_{\mathcal{X}_i}(\mathbf{x}_0 - \bar{\mathbf{x}}_{0,i})][(\mathbf{h} - \bar{\mathbf{h}}_i) - \mathbf{W}_{\mathcal{X}_i}(\mathbf{x}_0 - \bar{\mathbf{x}}_{0,i})]^T] \psi(\mathcal{X}_i) \right\} \\ &= \sum_{i=1}^v \left[\text{tr} \{ \mathbf{W}_{\mathcal{X}_i} \mathbf{C}_{\mathbf{x}_0\mathbf{x}_0|\mathcal{X}_i} \mathbf{W}_{\mathcal{X}_i}^T \} - \text{tr} \{ \mathbf{W}_{\mathcal{X}_i} \mathbf{C}_{\mathbf{x}_0\mathbf{h}|\mathcal{X}_i} \} - \text{tr} \{ \mathbf{C}_{\mathbf{h}\mathbf{x}_0|\mathcal{X}_i} \mathbf{W}_{\mathcal{X}_i}^T \} + \text{tr} \{ \mathbf{C}_{\mathbf{h}\mathbf{h}|\mathcal{X}_i} \} \right] \psi(\mathcal{X}_i), \end{aligned} \quad (29)$$

where $\mathbf{C}_{\mathbf{h}\mathbf{h}|\mathcal{X}_i}$ is the conditional covariance matrix of $\mathbf{h}\mathbf{h}^T$ when \mathbf{x}_0 is located at \mathcal{X}_i . Then, plugging (26) into (29) further produces

$$J_{\text{DL}} = \sum_{i=1}^v \left[\text{tr} \{ \mathbf{C}_{\mathbf{h}\mathbf{h}|\mathcal{X}_i} \} - \text{tr} \{ \mathbf{C}_{\mathbf{h}\mathbf{x}_0|\mathcal{X}_i} \mathbf{C}_{\mathbf{x}_0\mathbf{x}_0|\mathcal{X}_i}^{-1} \mathbf{C}_{\mathbf{x}_0\mathbf{h}|\mathcal{X}_i} \} \right] \psi(\mathcal{X}_i). \quad (30)$$

Considering $\mathbf{h} = \frac{1}{\tau}(\mathbf{x}_0 - \mathbf{n})$, J_{DL} can be expanded as

$$\begin{aligned}
J_{\text{DL}} &= \sum_{i=1}^v \text{tr}\{\mathbf{C}_{\mathbf{h}\mathbf{h}|\mathcal{X}_i} - \mathbf{C}_{\mathbf{x}_0\mathbf{x}_0|\mathcal{X}_i} - \mathbf{C}_{\mathbf{n}\mathbf{x}_0|\mathcal{X}_i} - \mathbf{C}_{\mathbf{x}_0\mathbf{n}|\mathcal{X}_i} + \mathbf{C}_{\mathbf{n}\mathbf{x}_0|\mathcal{X}_i} \mathbf{C}_{\mathbf{x}_0\mathbf{x}_0|\mathcal{X}_i}^{-1} \mathbf{C}_{\mathbf{x}_0\mathbf{n}|\mathcal{X}_i}\} \psi(\mathcal{X}_i) \\
&= \text{tr}\{\mathbf{R}\} - \text{tr}\{(\mathbf{R}_{\mathbf{x}_0\mathbf{x}_0} - \mathbf{R}_{\mathbf{n}\mathbf{x}_0} - \mathbf{R}_{\mathbf{x}_0\mathbf{n}})\} - \sum_{i=1}^v \text{tr}\{\mathbf{C}_{\mathbf{n}\mathbf{x}_0|\mathcal{X}_i} \mathbf{C}_{\mathbf{x}_0\mathbf{x}_0|\mathcal{X}_i}^{-1} \mathbf{C}_{\mathbf{x}_0\mathbf{n}|\mathcal{X}_i}\} \psi(\mathcal{X}_i) \\
&= J_{\text{LS}} - \sum_{i=1}^v \text{tr}\{\mathbf{C}_{\mathbf{n}\mathbf{x}_0|\mathcal{X}_i} \mathbf{C}_{\mathbf{x}_0\mathbf{x}_0|\mathcal{X}_i}^{-1} \mathbf{C}_{\mathbf{x}_0\mathbf{n}|\mathcal{X}_i}\} \psi(\mathcal{X}_i), \tag{31}
\end{aligned}$$

where $\mathbf{R}_{\mathbf{x}_0\mathbf{x}_0} = \mathbb{E}(\mathbf{x}_0\mathbf{x}_0^T)$ and $\mathbf{R}_{\mathbf{x}_0\mathbf{n}} = \mathbb{E}(\mathbf{x}_0\mathbf{n}^T)$ with $\mathbf{R}_{\mathbf{x}_0\mathbf{n}} = \mathbf{R}_{\mathbf{n}\mathbf{x}_0}^T$. Since $\text{tr}\{\mathbf{C}_{\mathbf{n}\mathbf{x}_0|\mathcal{X}_i} \mathbf{C}_{\mathbf{x}_0\mathbf{x}_0|\mathcal{X}_i}^{-1} \mathbf{C}_{\mathbf{x}_0\mathbf{n}|\mathcal{X}_i}\}$ in (31) is positive, the MSE of the DL estimator is lower than that of the LS estimator when m is sufficiently large.

To compare J_{DL} and J_{LMMSE} , we need to compute the gap between the LMMSE or the DL estimator and the MMSE estimator first. According to Bayesian theorem, the MMSE estimator is optimal under the criterion of minimizing the estimation MSE and its estimate is the conditional mean [24] shown as follows

$$\hat{\mathbf{h}}_{\text{MMSE}} = \mathbb{E}\{\mathbf{h}|\mathbf{x}_0\}. \tag{32}$$

To measure how close J_{DL} and J_{LMMSE} are to the MSE of $\hat{\mathbf{h}}_{\text{MMSE}}$, we introduce another way to express the MSE of an estimator. Let $\hat{\mathbf{h}}$ be an arbitrary channel estimate given a received signal \mathbf{x}_0 . The estimation error at \mathbf{x}_0 after averaging the randomness of training samples can be written as

$$\begin{aligned}
\mathbb{E}_{\mathcal{Z}}\{\|\mathbf{h} - \hat{\mathbf{h}}\|_2^2\} &= (\|\mathbf{h}\|_2^2 - \|\hat{\mathbf{h}}_{\text{MMSE}}\|_2^2) + (\mathbb{E}_{\mathcal{Z}}\{\|\hat{\mathbf{h}}\|_2^2\} - \|\mathbb{E}_{\mathcal{Z}}\{\hat{\mathbf{h}}\}\|_2^2) \\
&\quad + (\|\mathbb{E}_{\mathcal{Z}}\{\hat{\mathbf{h}}\}\|_2^2 - 2\mathbf{h}^T \mathbb{E}_{\mathcal{Z}}\{\hat{\mathbf{h}}\} - \|\hat{\mathbf{h}}_{\text{MMSE}}\|_2^2). \tag{33}
\end{aligned}$$

The expectation of \mathbf{h} conditioned on \mathbf{x}_0 is computed as

$$\mathbb{E}_{\mathbf{h}|\mathbf{x}_0} \mathbb{E}_{\mathcal{Z}}\{\|\mathbf{h} - \hat{\mathbf{h}}\|_2^2\} = \mathbf{C}_{\mathbf{h}|\mathbf{x}_0} + \mathbf{C}_{\hat{\mathbf{h}}} + \|\mathbb{E}_{\mathcal{Z}}\{\hat{\mathbf{h}}\} - \hat{\mathbf{h}}_{\text{MMSE}}\|_2^2, \tag{34}$$

where $\mathbf{C}_{\mathbf{h}|\mathbf{x}_0}$ is the covariance matrix of the posterior probability density function (PDF) $p(\mathbf{h}|\mathbf{x}_0)$ and $\mathbf{C}_{\hat{\mathbf{h}}}$ is the covariance matrix of the estimate $\hat{\mathbf{h}}$. The first term $\mathbf{C}_{\mathbf{h}|\mathbf{x}_0}$ is the estimation error of the MMSE estimator given \mathbf{x}_0 . The second term and the third term are variance and bias, respectively. The bias term is the squared difference between the average of $\hat{\mathbf{h}}$ and $\hat{\mathbf{h}}_{\text{MMSE}}$. Then, the variance term is simply the variance of $\hat{\mathbf{h}}$ around its mean.

Based on (34), we rewrite the estimation error of the LMMSE estimator at \mathbf{x}_0 as

$$J_{\text{LMMSE}}(\mathbf{x}_0) = \mathbf{C}_{\mathbf{h}|\mathbf{x}_0} + \|\hat{\mathbf{h}}_{\text{LMMSE}} - \hat{\mathbf{h}}_{\text{MMSE}}\|_2^2. \tag{35}$$

Specifically, if \mathbf{h} is Gaussian for the linear model in (1), $\hat{\mathbf{h}}_{\text{MMSE}}$ is simply equivalent to $\hat{\mathbf{h}}_{\text{LMMSE}}$. Thus, the bias in (35) is equal to zero. Since $\mathbf{C}_{\mathbf{h}|\mathbf{x}_0} = \mathbf{C}_{\mathbf{h}\mathbf{h}} - \mathbf{C}_{\mathbf{h}\mathbf{x}_0} \mathbf{C}_{\mathbf{x}_0\mathbf{x}_0}^{-1} \mathbf{C}_{\mathbf{x}_0\mathbf{h}}$ is independent of \mathbf{x} and $J_{\text{LMMSE}} = \mathbf{C}_{\mathbf{h}|\mathbf{x}_0}$, the expectation of $J_{\text{LMMSE}}(\mathbf{x}_0)$ over \mathbf{x}_0 is J_{LMMSE} .

Similar to (35), the estimation error of the DL estimator given an input $\mathbf{x}_0 \in \mathcal{X}_i$ can be computed as

$$J_{\text{DL}}(\mathbf{x}_0) = \mathbb{E}\{\|\mathbf{h}\|_2^2 | \mathbf{x}_0 \in \mathcal{X}_i\} - \|\hat{\mathbf{h}}_{\text{MMSE}}\|_2^2 + \|\hat{\mathbf{h}}_{\text{DL},i} - \hat{\mathbf{h}}_{\text{MMSE}}\|_2^2, \quad (36)$$

where $\mathbb{E}\{\|\mathbf{h}\|_2^2 | \mathbf{x}_0 \in \mathcal{X}_i\}$ is the conditional expectation over the PDF $p(\mathbf{h}|\mathbf{x}_0 \in \mathcal{X}_i)$. The expectation of $J_{\text{DL}}(\mathbf{x}_0)$ over \mathbf{x}_0 is given by

$$\begin{aligned} J_{\text{DL}} &= \mathbb{E}_{\mathbf{x}_0} \left\{ \sum_{i=1}^v \mathbb{E}\{\|\mathbf{h}\|_2^2 | \mathbf{x}_0 \in \mathcal{X}_i\} \psi(\mathcal{X}_i) - \|\hat{\mathbf{h}}_{\text{MMSE}}\|_2^2 \right\} + \sum_{i=1}^v \mathbb{E}_{\mathbf{x}_0 \in \mathcal{X}_i} \left\{ \|\hat{\mathbf{h}}_{\text{DL},i} - \hat{\mathbf{h}}_{\text{MMSE}}\|_2^2 \right\} \psi(\mathcal{X}_i) \\ &= J_{\text{LMMSE}} + \sum_{i=1}^v \mathbb{E}_{\mathbf{x}_0 \in \mathcal{X}_i} \left\{ \|\hat{\mathbf{h}}_{\text{DL},i} - \hat{\mathbf{h}}_{\text{MMSE}}\|_2^2 \right\} \psi(\mathcal{X}_i). \end{aligned} \quad (37)$$

Since the bias term $\|\hat{\mathbf{h}}_{\text{DL},i} - \hat{\mathbf{h}}_{\text{MMSE}}\|_2^2$ in (37) is non-negative, J_{LMMSE} is always smaller than J_{DL} in linear systems. Therefore, the expected loss J_{DL} is upper and lower bounded by

$$J_{\text{LMMSE}} \leq J_{\text{DL}} \leq J_{\text{LS}}. \quad (38)$$

Remark 2: In summary, the LS and LMMSE estimators are more suitable to linear systems due to their simplicity and accuracy. Owing to no assumption about underlying signal model, the DL estimator has to take sufficiently large training data to learn an effective estimator from scratch, which is relatively inefficient compared to LS or LMMSE estimators. In fact, we can retrain a learned DL estimator that is originally trained at similar scenarios to accelerate the training process as what the transfer learning has done in image processing [32]. Furthermore, different from the LS and LMMSE estimators that can be applied to the whole input space, the learned DL estimator can only make valid estimate for the inputs that are restricted to regions where training samples are not empty and would behaves randomly outside these regions. In general, this limitation has a little impact on the performance of the DL estimator when training data is accurate since the probabilities that \mathbf{x}_0 falls into the regions without training samples are negligible. However, if the statistics of training data do not match with real channels, such limitation would lead to serious issues, as will be discussed later.

Remark 3: Though the LMMSE estimator outperforms the DL estimator from the inequality in (38) when both \mathbf{h} and \mathbf{n} are Gaussian, the bias term $\|\hat{\mathbf{h}}_{\text{DL},i} - \hat{\mathbf{h}}_{\text{MMSE}}\|_2^2$ in (37) is a very small value as analyzed in the next subsection. The difference between the estimation performance of the LMMSE and the DL estimators is negligible and J_{DL} is quite equal to J_{LMMSE} as illustrated in the later simulations. When the distributions of \mathbf{h} and \mathbf{n} are non-Gaussian, it is difficult to derive an analytic form of $\hat{\mathbf{h}}_{\text{MMSE}}$

and the comparison between J_{DL} and J_{LMMSE} is not straightforward. Nevertheless, a unified performance assessment of the DL estimator will be presented in the next subsection.

Remark 4: Inequality (38) is also demonstrated by simulation results in [8] for channel estimation in OFDM systems. Therefore, many analytical results in this paper are applicable to channel estimation for a large range of communication systems.

C. Performance Assessment in Nonlinear Systems

In practice, wireless communication systems suffer from certain nonlinear effects, e.g., imperfection of PA and quantization error of ADC. It is hard to establish precise signal models in most nonlinear systems and the corresponding channel estimation is very challenging. The performance of the LS and LMMSE estimators would significantly degrade when deployed in nonlinear systems since the biases between the estimated channels derived from the linear estimators and the target channels are in general large. Nevertheless, the DL estimator does not restrict to any type of signal models or channel statistics and is able to build up a stable and precise model to estimate \mathbf{h} by making efficient use of training data. Such a property makes the DL estimator a great choice for channel estimation in nonlinear systems.

In general, the theoretical framework in nonlinear communication systems is captured by the following statistical model

$$\mathbf{x}_0 = f_{NL}(\tau\mathbf{h} + \mathbf{n}), \quad (39)$$

where $f_{NL}(\cdot)$ denotes the nonlinear distortion imposed on the received signal. Specifically, the nonlinear model in (39) reduces to the linear model (1) if $f_{NL}(\cdot)$ is a linear function. Therefore, the following analysis on the performance of the DL estimator can be applied equally to linear systems.

Though $f_{NL}(\cdot)$ is generally unable to manipulate, the optimal estimate of \mathbf{h} can still be provided by the MMSE estimator in (35). Unfortunately, the explicit expression of $\hat{\mathbf{h}}_{MMSE}$ is impossible to obtain in most nonlinear cases. Hence, the LMMSE estimator is still used for channel estimation in nonlinear systems before the advent of the DL estimator. When applying the LMMSE estimator to (39), we obtain

$$\hat{\mathbf{h}}_{LM-NL} = \mathbf{C}_{\mathbf{h}\mathbf{x}_0} \mathbf{C}_{\mathbf{x}_0\mathbf{x}_0}^{-1} [\mathbf{x}_0 - \mathbb{E}(\mathbf{x}_0)]. \quad (40)$$

Using the LMMSE estimator is simple but may have a relatively low accuracy. There exit two major problems that affect the performance of the LMMSE estimator. Firstly, it is difficult to acquire accurate channel statistics due to complexity and uncertainty of nonlinear systems. Secondly, the LMMSE estimator is only best suited to linear systems. The system error of fitting nonlinear objective function with a linear estimator is big. Either way, the LMMSE estimator is not a good option for channel estimation in nonlinear systems.

On the other hand, the DL estimator is far more expressive than the LMMSE estimator and is more suitable to deploy in nonlinear systems. Similar to linear systems, the DL estimate of \mathbf{h} in nonlinear systems is directly derived from a local linear function in (23). Given an input point $\mathbf{x}_0 \in \mathcal{X}_i$, the estimated channel of the DL estimator with a large number of training samples is given by

$$\hat{\mathbf{h}}_{\text{DL-NL},i} = \mathbf{C}_{\mathbf{h}\mathbf{x}_0|\mathcal{X}_i} \mathbf{C}_{\mathbf{x}_0\mathbf{x}_0|\mathcal{X}_i}^{-1} (\mathbf{x}_0 - \bar{\mathbf{x}}_{0,i}) + \bar{\mathbf{h}}_i \quad \forall \mathbf{x}_0 \in \mathcal{X}_i. \quad (41)$$

To compare the estimation MSEs of the LMMSE and DL estimators, we apply the decomposition in (34) to assess their estimation performance. For the LMMSE estimator, its MSE in nonlinear systems can be decomposed into

$$J_{\text{LM-NL}} = \mathbb{E}_{\mathbf{x}_0} \{ \mathbf{C}_{\mathbf{h}|\mathbf{x}_0} \} + \mathbb{E}_{\mathbf{x}_0} \{ \| \hat{\mathbf{h}}_{\text{LM-NL}} - \hat{\mathbf{h}}_{\text{MMSE}} \|^2 \}, \quad (42)$$

where $\mathbb{E}_{\mathbf{x}_0} \{ \mathbf{C}_{\mathbf{h}|\mathbf{x}_0} \}$ is the estimation MSE of the MMSE estimator and $\| \hat{\mathbf{h}}_{\text{LM-NL}} - \hat{\mathbf{h}}_{\text{MMSE}} \|^2$ is the squared bias. Unlike the linear systems, $\hat{\mathbf{h}}_{\text{MMSE}}$ is typically nonlinear in \mathbf{x}_0 and the bias $\| \hat{\mathbf{h}}_{\text{LM-NL}} - \hat{\mathbf{h}}_{\text{MMSE}} \|^2$ in (42) is no longer zero. To reduce the model bias, we have to enlarge the class of models representable by an estimator to a richer collection such that it does not underfit the signal models in nonlinear systems. Clearly, the DL estimator is a good candidate for these requirements.

Based on the decomposition in (34), we compute the estimation MSE of the DL estimator as

$$J_{\text{DL-NL}} = \mathbb{E}_{\mathbf{x}_0} \{ \mathbf{C}_{\mathbf{h}|\mathbf{x}_0} \} + \sum_{i=1}^v \mathbb{E}_{\mathbf{x}_0 \in \mathcal{X}_i} \{ \| \hat{\mathbf{h}}_{\text{DL-NL},i} - \hat{\mathbf{h}}_{\text{MMSE}} \|^2 \} \psi(\mathcal{X}_i), \quad (43)$$

where $\| \hat{\mathbf{h}}_{\text{DL-NL},i} - \hat{\mathbf{h}}_{\text{MMSE}} \|^2$ denotes the squared bias. Instead of using a global linear function $\hat{\mathbf{h}}_{\text{LM-NL}}$ to approximate $\hat{\mathbf{h}}_{\text{MMSE}}$ in (42), the DL estimator divides the input domain into v regions, as in (10), and applies a set of linear functions $\hat{\mathbf{h}}_{\text{DL-NL},i}$ in (41) to approximate $\hat{\mathbf{h}}_{\text{MMSE}}$.

The main difference between $J_{\text{LM-NL}}$ and $J_{\text{DL-NL}}$ is the model bias between these two estimators and the MMSE estimator. Considering that the analytic form of $\hat{\mathbf{h}}_{\text{MMSE}}$ is not available in nonlinear systems, the bias terms of $J_{\text{LM-NL}}$ and $J_{\text{DL-NL}}$ are incomparable, and we can not derive the firm conclusion as in (38) on the estimation performance assessment about the LMMSE and DL estimators from the biases. Nevertheless, since the DL estimator is a universal approximator to a large family of functions, intuitively, it can fit to $\hat{\mathbf{h}}_{\text{MMSE}}$ better than the LMMSE estimator. To support this idea, we will show that the target function that the DL estimator approaches to, under large m , is exactly $\hat{\mathbf{h}}_{\text{MMSE}}$.

Firstly, we prove that the minimization of J_{emp} in (14) is equivalent to minimizing $J_{\text{DL-NL}}$ as m gets large. Let Θ be the parameter space of θ . Denote $\hat{\theta}_0$ and $\hat{\theta}_m$ as the optimal variables by minimizing $J_{\text{DL-NL}}$, and we obtain

$$\hat{\theta}_0 = \min_{\theta \in \Theta} J_{\text{NL-DL}} = \mathbb{E}_z \{ \| \mathbf{h} - g(\mathbf{x}_0, \theta) \|^2 \} \quad (44)$$

and J_{emp}

$$\hat{\theta}_m = \min_{\theta \in \Theta} J_{emp} = \frac{1}{m} \sum_{z_i \in Z_m} \|\mathbf{h}_i - g(\mathbf{x}_{0,i}, \theta)\|_2^2, \quad (45)$$

respectively. For the DL estimator built on ReLU DNN, $\hat{\mathbf{h}}_{DL,i}$ in (23) asymptotically approaches to $\hat{\mathbf{h}}_{DL-NL,i}$ in (41) as m gets large and we have $\hat{\theta}_m \xrightarrow{a.s.} \hat{\theta}_0$. Denote by $J(\hat{\theta}_0)$ and $J_m(\hat{\theta}_m)$ the minimum values of J_{DL-NL} and J_{emp} , respectively.

Proposition 1: Since $\hat{\theta}_m \xrightarrow{a.s.} \hat{\theta}_0$ as $m \rightarrow \infty$, there is

$$J_m(\hat{\theta}_m) \xrightarrow{a.s.} J(\hat{\theta}_0). \quad (46)$$

Proof: Substituting $\hat{\theta}_m$ and $\hat{\theta}_0$ into J_{DL} and J_{emp} yields

$$J(\hat{\theta}_0) = \mathbb{E}_z\{\|\mathbf{h} - g(\mathbf{x}_0, \hat{\theta}_0)\|_2^2\} \quad (47)$$

and

$$J_m(\hat{\theta}_m) = \frac{1}{m} \sum_{z_i \in Z_m} \|\mathbf{h}_i - g(\mathbf{x}_{0,i}, \hat{\theta}_m)\|_2^2, \quad (48)$$

respectively. Since $\hat{\theta}_m \xrightarrow{a.s.} \hat{\theta}_0$, we obtain

$$J_m(\hat{\theta}_m) \xrightarrow{a.s.} J_m(\hat{\theta}_0). \quad (49)$$

When m is sufficiently large, there is

$$J_m(\hat{\theta}_0) \xrightarrow{a.s.} J(\hat{\theta}_0) \quad (50)$$

according to the law of large numbers [30]. ■

Secondly, we will show that the target function of the DL estimator by minimizing J_{DL-NL} is $\hat{\mathbf{h}}_{MMSE}$. Replacing $\hat{\mathbf{h}}_{DL,i}$ with $g(\mathbf{x}, \theta)$ in J_{DL-NL} , we can rewrite J_{DL} as

$$J_{DL-NL} = \int [\mathbf{C}_{\mathbf{h}|\mathbf{x}_0} + \|g(\mathbf{x}_0, \theta) - \hat{\mathbf{h}}_{MMSE}\|^2] \psi_{\mathbf{x}_0}(\mathbf{x}_0) d\mathbf{x}_0, \quad (51)$$

where $\psi_{\mathbf{x}_0}(\mathbf{x}_0)$ is the PDF of \mathbf{x}_0 . The minimization of J_{DL-NL} w.r.t. θ can be reformulated as

$$\min_{\theta \in \Theta} \int \|g(\mathbf{x}_0, \theta) - \hat{\mathbf{h}}_{MMSE}\|^2 \psi_{\mathbf{x}_0}(\mathbf{x}_0) d\mathbf{x}_0, \quad (52)$$

i.e., the target function $g(\mathbf{x}_0, \theta)$ approximates to is $\hat{\mathbf{h}}_{MMSE}$.

Following Proposition 1, the target function of the DL estimator by minimizing J_{emp} as $m \rightarrow \infty$ is also $\hat{\mathbf{h}}_{MMSE}$. Meanwhile, according to Theorem 2.3 in [29], the DL estimator power by a ReLU DNN is a universal approximator to a large family of functions. Therefore, if the underlying network structure is reasonably configured and $\hat{\mathbf{h}}_{MMSE}$ satisfies the requirements of Theorem 2.3 in [29], then

$g(\mathbf{x}_0, \theta)$ would approach to $\hat{\mathbf{h}}_{\text{MMSE}}$ with any precision from a theoretical perspective. In this case, the bias $\|\hat{\mathbf{h}}_{\text{DL-NL},i} - \hat{\mathbf{h}}_{\text{MMSE}}\|^2$ in (43) becomes an arbitrarily small value and we have

$$J_{\text{DL-NL}} \approx \mathbb{E}_{\mathbf{x}_0} \{ \mathbf{C}_{\mathbf{h}|\mathbf{x}_0} \}. \quad (53)$$

Remark 5: Combining Proposition 1 and Theorem 2.3 in [29], we show that the estimated channel of DL estimator with the underlying ReLU DNN structure asymptotically approaches to $\hat{\mathbf{h}}_{\text{MMSE}}$ as m gets large. Such a result provides a theoretical insight into the excellent performance of the DL estimator when deployed in linear and nonlinear systems. It is hopeful to introduce the DL estimator to combat the nonlinear detrimental effects brought by the imperfection of PA and the quantification error of ADC.

Remark 6: Since the LMMSE estimator can model only a single class of functions, it is vulnerable to environmental disturbance and has not enough capacity to model the nonlinearities of real systems. On the other hand, the DL estimator is more intelligent to find out a lot of hidden factors influencing the estimation accuracy by iteratively learning the training data and then continually adjusting itself to best fit the training data. In this way, the DL estimator can asymptotically evolve to an effective estimator during the training process. Therefore, if the model bias of the LMMSE estimator is relatively large, the DL estimator is very likely to outperform the LMMSE estimator for channel estimation.

Remark 7: Considering that the analytic form of the LS estimator is difficult to calculate in nonlinear systems and the LMMSE estimator is the best linear estimator for any distribution with the same first two moments [33], we omit the analysis on the estimation performance of the LS estimator in nonlinear systems.

V. ROBUSTNESS OF CHANNEL ESTIMATION TO MISMATCHED INFORMATION

The optimality of the LMMSE and DL estimator is built on the perfect knowledge of channel statistics and accurate training data, respectively, while it is a typical problem that the channel covariance matrix \mathbf{R} is not perfectly known or the statistics of training data do not match the deployed environments. In this section, we analyze channel estimation with inaccurate channel statistics and mismatched training data in linear systems and show how these imperfections affect the performance of the LMMSE and DL estimators.

A. LMMSE Estimator

Denote the channel covariance matrix used by the LMMSE estimator as $\mathbf{R}_1 = \mathbf{R} + \mathbf{\Omega}$, where $\mathbf{\Omega}$ is a $t_0 \times t_0$ Hermitian random error matrix independent of \mathbf{R} . Replacing \mathbf{R} with \mathbf{R}_1 in (4), the LMMSE estimator under inaccurate channel statistic can be expressed as

$$\hat{\mathbf{h}}_{\text{LM-ER}} = \mathbf{R}_1 (\mathbf{R}_1 + \sigma_n^2 \mathbf{I}_{t_0})^{-1} \mathbf{x}_0, \quad (54)$$

and the corresponding MSE is given by

$$\begin{aligned} J_{\text{LM-ER}} &= \mathbb{E}(\text{tr}\{(\mathbf{h} - \hat{\mathbf{h}}_{\text{LM-ER}})(\mathbf{h} - \hat{\mathbf{h}}_{\text{LM-ER}})^T\}) \\ &= \text{tr}\left\{\left(\mathbf{R}_1^{-1} + \frac{1}{\sigma_n^2}\mathbf{I}_{t_0}\right)^{-1} - \mathbf{\Pi}\mathbf{\Omega}\mathbf{\Pi}^T\right\}, \end{aligned} \quad (55)$$

where $\mathbf{\Pi} = \mathbf{I}_{t_0} - \mathbf{R}_1(\mathbf{R}_1 + \sigma_n^2\mathbf{I}_{t_0})^{-1}$.

It is difficult to figure out how $\mathbf{\Omega}$ affects the estimation accuracy of the LMMSE estimator directly from (55). Since the channels between different received antennas are asymptotically uncorrelated when t_0 gets large [34], we take the uncorrelated channel as an example to analyze the influence of $\mathbf{\Omega}$ on $J_{\text{LM-ER}}$.

Suppose that the covariance matrix of \mathbf{h} is diagonal with $\mathbf{R} = \sigma^2\mathbf{I}_{t_0}$, where σ^2 is element-wise variance. Moreover, assume that $\mathbf{\Omega}$ can be decomposed into

$$\mathbf{\Omega} = \mathbf{U}\mathbf{\Sigma}\mathbf{U}^T, \quad (56)$$

where \mathbf{U} is a $t_0 \times t_0$ eigenvector matrix and $\mathbf{\Sigma}$ is a $t_0 \times t_0$ eigenvalue matrix. Substituting $\mathbf{R} = \sigma^2\mathbf{I}_{t_0}$ and (56) into (54), we can rewrite $J_{\text{LM-ER}}$ as

$$J_{\text{LM-ER}} = J_{\text{LMMSE}} + \sum_{i=1}^{t_0} \frac{\sigma_{e,i}^4 \sigma_n^4 t_0}{(\sigma^2 + \sigma_{e,i}^2 + \sigma_n^2)^2 (\sigma^2 + \sigma_n^2)}, \quad (57)$$

where $\sigma_{e,i}^2$ is the i -th diagonal element of $\mathbf{\Sigma}$. Reversely, if $\mathbf{R} = \mathbf{R}_1 + \mathbf{\Omega}$ and $\mathbf{R} = \sigma^2\mathbf{I}_{t_0}$, then we can still obtain the same form of $J_{\text{LM-ER}}$ in (57).

Remark 8: According to (57), $J_{\text{LM-ER}}$ is always larger than J_{LMMSE} and is increased with $\sigma_{e,i}^2$. The performance of the LMMSE estimator is mainly determined by the accuracy of \mathbf{R} . In contrast, the DL estimator needs to know neither the exact signal model nor the information of \mathbf{R} to estimate \mathbf{h} . Namely, whether \mathbf{R} is accurate or not does not affect the accuracy of the DL estimator. Hence, the DL estimator will outperform the LMMSE estimator if $\sigma_{e,i}^2$ exceeds certain threshold, i.e., $J_{\text{LM-ER}} \geq J_{\text{DL}}$.

B. DL Estimator

Different from the LMMSE estimator, the DL estimator is data-driven and its performance is mainly determined by how well the training data matches the working environment. Mismatched training data would lead to significant performance degradation. Furthermore, the DL estimator is only effective in a small percentage of partitioned regions, where A_i is not empty. The negative effect of such limitation cannot be ignored when the training data is mismatched since the probability for \mathbf{x}_0 located at regions with empty training sample is no longer close to zero. The computation on the estimation MSE of the DL estimator under inaccurate training data needs to be divided into two cases.

1) *Case 1*: Denote by \mathbf{h}_{er} the channel of inaccurate training data. In this case, \mathbf{h}_{er} distributes in a broader range than \mathbf{h} , and the corresponding statistical model of the training data can be described as

$$\mathbf{h}_{\text{er}} = \mathbf{h} + \boldsymbol{\varepsilon}, \quad (58)$$

and

$$\mathbf{x}_{\text{er}} = \tau \mathbf{h}_{\text{er}} + \mathbf{n}, \quad (59)$$

where $\boldsymbol{\varepsilon}$ denotes the $t_0 \times 1$ zero mean random error vector that is independent of \mathbf{h} and has covariance matrix $\boldsymbol{\Omega}_\varepsilon = \mathbb{E}\{\boldsymbol{\varepsilon}\boldsymbol{\varepsilon}^T\}$.

In Case 1, the probability that \mathbf{x}_0 locates at regions without training samples is close to zero since \mathbf{x}_{er} is more broadly distributed than \mathbf{x}_0 . The input-output pair in training set Z_m is transformed into $(\mathbf{x}_{\text{er},i}, \mathbf{h}_{\text{er},i})$ for $i \in \{1, \dots, m\}$, where $\mathbf{x}_{\text{er},i}$ and $\mathbf{h}_{\text{er},i}$ are with the same distributions as \mathbf{x}_{er} and \mathbf{h}_{er} , respectively. After training, the DL estimator is assumed to follow the same configurations in Section III-A. The input space is partitioned into a set of v linear regions $\{\mathcal{X}_1, \dots, \mathcal{X}_v\}$ as the scheme in (10). The set index of samples in \mathcal{X}_i is denoted by A_i with probabilities $(\psi(\mathcal{X}_1), \dots, \psi(\mathcal{X}_v))$.

Hence, given an input $\mathbf{x}_0 \in \mathcal{X}_i$, the estimated channel from the DL estimator under mismatched training data and sufficiently large m is written as

$$\hat{\mathbf{h}}_{\text{DL-ER},i} = \mathbf{C}_{\mathbf{h}_{\text{er}}\mathbf{x}_{\text{er}}|\mathcal{X}_i} \mathbf{C}_{\mathbf{x}_{\text{er}}\mathbf{x}_{\text{er}}|\mathcal{X}_i}^{-1} (\mathbf{x}_0 - \bar{\mathbf{x}}_{\text{er},i}) + \bar{\mathbf{h}}_{\text{er},i} \quad \forall \mathbf{x}_0 \in \mathcal{X}_i, \quad (60)$$

where $\mathbf{C}_{\mathbf{h}_{\text{er}}\mathbf{x}_{\text{er}}|\mathcal{X}_i}$ is the conditional cross-covariance of $\mathbf{h}_{\text{er}}\mathbf{x}_{\text{er}}^T$, $\mathbf{C}_{\mathbf{x}_{\text{er}}\mathbf{x}_{\text{er}}|\mathcal{X}_i}$ is the conditional covariance of $\mathbf{x}_{\text{er}}\mathbf{x}_{\text{er}}^T$, $\bar{\mathbf{x}}_{\text{er},i} = \mathbb{E}\{\mathbf{x}_{\text{er}}|\mathbf{x}_{\text{er}} \in \mathcal{X}_i\}$, and $\bar{\mathbf{h}}_{\text{er},i} = \mathbb{E}\{\mathbf{h}_{\text{er}}|\mathbf{x}_{\text{er}} \in \mathcal{X}_i\}$. The MSE of the DL estimator is then computed as

$$J_{\text{DL-ER}} = \mathbf{C}_{\mathbf{h}|\mathbf{x}_0} + \sum_{i=1}^v \mathbb{E}_{\mathbf{x}_0 \in \mathcal{X}_i} \{ \|\hat{\mathbf{h}}_{\text{DL-ER},i} - \hat{\mathbf{h}}_{\text{MMSE}}\|^2 \} \psi(\mathcal{X}_i). \quad (61)$$

From Section IV-C, the target estimator that the DL estimator approaches to as m gets large is the MMSE estimator. Therefore, the target channel for $\hat{\mathbf{h}}_{\text{DL-ER},i}$ is the estimated channel of the MMSE estimator derived from (59), which is given by

$$\hat{\mathbf{h}}_{\text{MM-ER}} = \mathbf{C}_{\mathbf{h}_{\text{er}}\mathbf{x}_{\text{er}}} \mathbf{C}_{\mathbf{x}_{\text{er}}\mathbf{x}_{\text{er}}}^{-1} \mathbf{x}_0, \quad (62)$$

where $\mathbf{C}_{\mathbf{h}_{\text{er}}\mathbf{x}_{\text{er}}}$ is the cross-covariance of $\mathbf{h}_{\text{er}}\mathbf{x}_{\text{er}}^T$, and $\mathbf{C}_{\mathbf{x}_{\text{er}}\mathbf{x}_{\text{er}}}$ is the covariance of $\mathbf{x}_{\text{er}}\mathbf{x}_{\text{er}}^T$. If the DL estimator is properly trained and m is sufficiently, then we have $\hat{\mathbf{h}}_{\text{DL-ER},i} \approx \hat{\mathbf{h}}_{\text{MM-ER}}$ for $\mathbf{x}_0 \in \mathcal{X}_i$ according to Theorem 2.3 in [29]. Substituting (62) into (61) yields

$$J_{\text{DL-ER}} \approx \mathbf{C}_{\mathbf{h}|\mathbf{x}_0} + \mathbb{E}_{\mathbf{x}_0} \{ \|\mathbf{C}_{\mathbf{h}_{\text{er}}\mathbf{x}_{\text{er}}} \mathbf{C}_{\mathbf{x}_{\text{er}}\mathbf{x}_{\text{er}}}^{-1} - \mathbf{C}_{\mathbf{h}\mathbf{x}_0} \mathbf{C}_{\mathbf{x}_0\mathbf{x}_0}^{-1} \mathbf{x}_0\|^2 \}. \quad (63)$$

Similar to $J_{\text{LM-ER}}$ in (57), how ε affects $J_{\text{DL-ER}}$ is difficult to justify from (63). To provide some insight into the influence of the inaccurate training data on the DL estimator, we assume that $\mathbf{R} = \sigma^2 \mathbf{I}_{t_0}$. Moreover, the covariance matrix, $\mathbf{\Omega}_\varepsilon$, can be decomposed into

$$\mathbf{\Omega}_\varepsilon = \mathbf{U}_\varepsilon \mathbf{\Sigma}_\varepsilon \mathbf{U}_\varepsilon^T, \quad (64)$$

where \mathbf{U}_ε is the $t_0 \times t_0$ eigenvector matrix and $\mathbf{\Sigma}_\varepsilon$ is the $t_0 \times t_0$ eigenvalue matrix. Substituting $\mathbf{R} = \sigma^2 \mathbf{I}_{t_0}$ and (64) into (63), we have

$$J_{\text{DL-ER}} \approx J_{\text{LMMSE}} + \sum_{i=1}^{t_0} \frac{\sigma_{\varepsilon,i}^4 \sigma_n^4}{(\sigma^2 + \sigma_{\varepsilon,i}^2 + \sigma_n^2)^2 (\sigma^2 + \sigma_n^2)}, \quad (65)$$

where $\sigma_{\varepsilon,i}^2$ is the i -th diagonal element of $\mathbf{\Sigma}_\varepsilon$. The obtained $J_{\text{DL-ER}}$ in (65) is similar to $J_{\text{LM-ER}}$ in (57) and would also increase with $\sigma_{\varepsilon,i}^2$, which quantifies the mismatch degree between training data and real systems.

2) *Case 2:* We consider that the input-output pair of training data is generated from the following statistical model

$$\mathbf{h} = \mathbf{h}_{\text{er}} + \varepsilon, \quad (66)$$

and

$$\mathbf{x}_{\text{er}} = \tau \mathbf{h}_{\text{er}} + \mathbf{n}. \quad (67)$$

Since \mathbf{x}_0 distributes in a broader range than \mathbf{x}_{er} , the probability that \mathbf{x}_0 locates at regions without training samples would be much higher than Case 1. The estimated channels of the DL estimator corresponding to the inputs at empty regions are totally random and unacceptable if the discrepancy between \mathbf{h} and \mathbf{h}_{er} is sufficiently large. In this situation, it is difficult to derive an analytic form of the estimation MSE and the DL estimator basically fails to provide a reliable estimate.

Remark 9: In Case 1, the DL estimator can well approximate $\hat{\mathbf{h}}_{\text{MM-ER}}$ and provide a stable estimate as the MMSE estimator. However, the limitation on the effective input range of the DL estimator is immensely magnified when training data is mismatched in the way of Case 2. Such limitation makes the DL estimator unable to provide a valid estimate in some cases. The LMMSE estimator, however, is designed over the whole input space, and therefore the error introduced by the discrepancy between \mathbf{R} and \mathbf{R}_1 is controllable no matter how $\mathbf{\Omega}$ varies.

Remark 10: The rapid changing of channel statistics is another challenging problem faced by the DL estimator. Pre-trained DL estimator is not good at responding to very sudden changes of channels and at performing the channel estimation in environments that it is not familiar with will probably fail miserably. Re-training the underlying network of the DL estimator is always time consuming and

TABLE I
THE COMPARISON OF THE LS, LMMSE, AND DL ESTIMATORS.

ESTIMATORS	MODEL	REQUIREMENT	INACCURATE INFORMATION
LS	LINEAR	NO	NO DEGRADATION
LMMSE	LINEAR	CHANNEL STATISTICS	CONTROLLABLE DEGRADATION
DL	PWL	TRAINING DATA	SIGNIFICANT DEGRADATION

computing intensive while the real systems may shift too quickly for the DL estimator to catch up. Hence, though the DL estimator has many advantages as a new technology, there also exists some shortcomings compared to conventional estimation methods due to the lack of expert knowledge. The comparison of these estimators is shown in Table I, and balancing the tradeoffs of these estimators is vital for channel estimation in practices [35].

VI. SIMULATION RESULTS

In this section, computer-aided simulation is conducted to provide further evidence and insights into the performance assessment of various estimators, which also verifies the advantages and disadvantages of using the DL estimator based on channel estimation.

A. Linear Systems

We firstly compare the MSEs using the LS, LMMSE, and DL estimators versus SNR under linear signal model (1) in Fig. 2(a). The channel, \mathbf{h} , is assumed to be Gaussian with zero mean and element-wise unit variance. The sizes of training and test sets are 20,000 and 5,000, respectively. The underlying network of the DL estimator has 4 layers and each layer has 40 neurons.

From the figure, the MSEs of the LMMSE and the DL estimators are almost overlapped in Fig. 2(a). Therefore, the bias term of J_{DL} in (37) is close to zero, and the DL estimator can well approximate $\hat{\mathbf{h}}_{LMMSE}$. Such a result demonstrates that the formula (53) is valid and $J_{DL} \approx J_{LMMSE}$ in linear systems. Moreover, both DL and LMMSE estimators outperform the LS estimator in Fig 2(a) as noted by (38).

Fig. 2(b) visualizes the MSEs of the DL estimator versus m for channel estimation under linear signal model (1) with SNR fixed. The LMMSE estimator derived under the same SNR is used as the benchmark. When m is small, the MSEs of the DL estimator are significantly larger than the MSEs of the LMMSE estimator. As m increases, all MSEs of the DL estimator derived at different SNRs

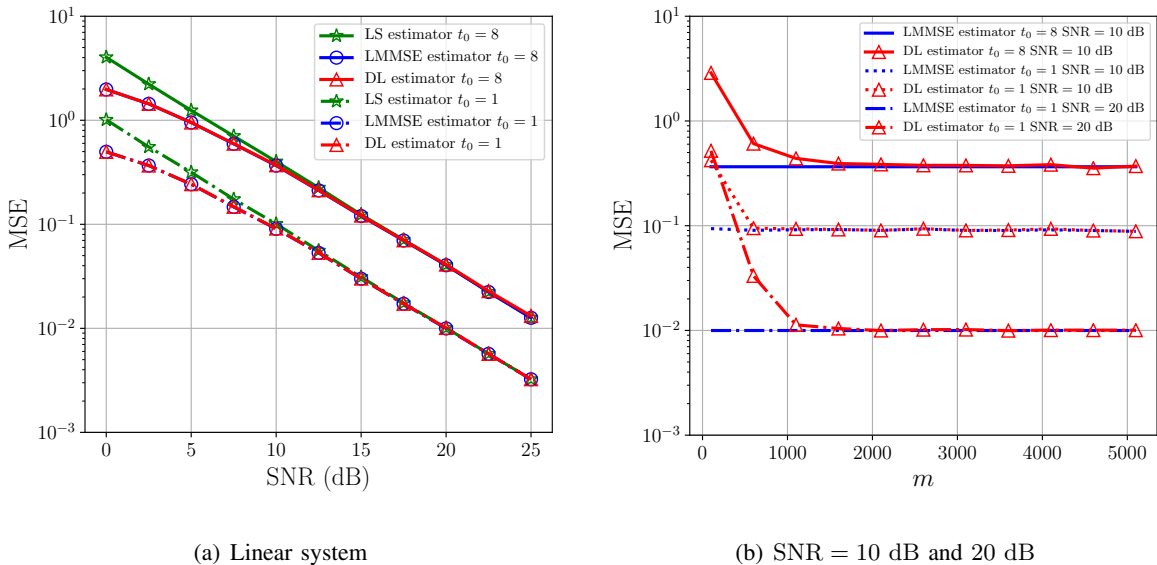


Fig. 2. (a) The MSE performance of the LS, LMMSE, and DL estimators versus SNR under linear signal model; (b) The MSE performance of the DL estimator versus m under linear signal model.

asymptotically approaches to the MSEs of the LMMSE estimator and remains unchanged at large m . Such result evidences the rationality of approximation taken in (25).

B. Nonlinear Systems

In this subsection, we evaluate the performance of the LMMSE and the DL estimators for channel estimation under a nonlinear signal model. Let $\mathbf{x}_{in} = \mathbf{h}\tau + \mathbf{n}$ and the following nonlinear model

$$x_i = x_{in,i} \left(1 + \left(\frac{x_{in,i}}{x_{sat}} \right)^{2\omega} \right)^{-\frac{1}{2\omega}} \quad (68)$$

is adopted to represent $f_{NL}(\cdot)$ in (39), where x_i and $x_{in,i}$ are the i -th elements of \mathbf{x}_0 in (39) and \mathbf{x}_{in} , respectively, for $i \in \{1, \dots, t_0\}$, x_{sat} is the saturation level, and ω is the smoothness factor. The other settings are the same with Section VI-A. The model in (68) is typically used by nonlinear signal detection caused by imperfection of PA and is commonly known as Rapp model [36]. Here, we apply such a model to the channels for an illustration of channel estimation in nonlinear systems.

Fig 3(a) shows the MSEs of the LMMSE and the DL estimators versus SNR under nonlinear model in (68), where the saturation level, x_{sat} , is fixed as 1.5 and the smoothness factor ω is set be 1. The performance of the LMMSE and DL estimators is close to each other at low SNRs since $\mathbb{E}_{\mathbf{x}_0}(\mathbf{C}_{\mathbf{h}|\mathbf{x}_0})$ of J_{LM-NL} and J_{DL-NL} in (42) and (43) are inversely related to SNR and dominates the overall MSEs. As the SNR increases, the percentages of $\mathbb{E}_{\mathbf{x}_0}(\mathbf{C}_{\mathbf{h}|\mathbf{x}_0})$ in J_{LM-NL} and J_{DL-NL} decrease and the bias terms

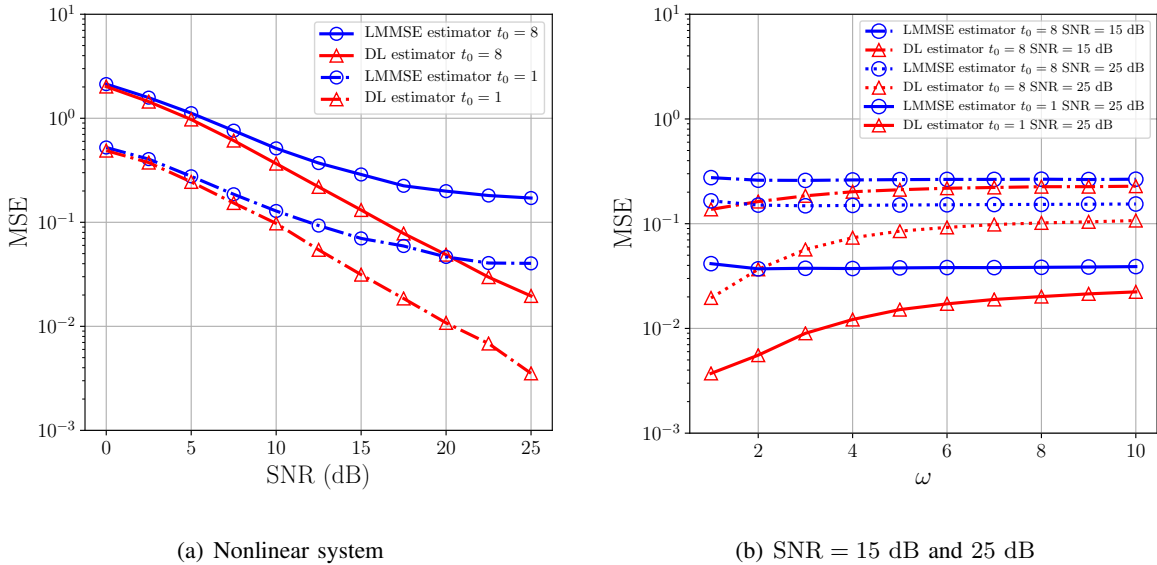


Fig. 3. The MSE performance of the LMMSE and the DL estimators versus SNR under nonlinear signal model; (b) The MSE performance of the LMMSE and the DL estimators versus ω under nonlinear signal model.

$\|\hat{\mathbf{h}}_{\text{DL-NL},i} - \hat{\mathbf{h}}_{\text{MMSE}}\|^2$ and $\|\hat{\mathbf{h}}_{\text{LM-NL}} - \hat{\mathbf{h}}_{\text{MMSE}}\|^2$ will take a larger percentage of $J_{\text{DL-NL}}$ and $J_{\text{LM-NL}}$, respectively. According to the analysis in Section IV-C, the bias of the DL estimator is significantly lower than that of the LMMSE estimator when applied in nonlinear systems. As a result, the performance gap between the LMMSE and the DL estimators grows increasingly wider as the SNR increases, which is in accordance with the result in (53).

Fig. 3(b) illustrates the MSEs of the LMMSE and the DL estimators versus ω for channel estimation under nonlinear model in (68) with SNR fixed and $x_{\text{sat}} = 1.5$. As discussed in [36], the nonlinearity of \mathbf{x}_0 in (68) before the saturation level decreases as ω increases. In Fig. 3(b), the performance gap between the LMMSE and the DL estimators also decreases with the increase of ω . Thus, the DL estimator is more capable of channel estimation in nonlinear systems while the performance of the LMMSE estimator degrades more significantly when more nonlinearities are imposed on the received signal. Moreover, the performance of the LMMSE and the DL estimators degrades when ω is large since the nonlinear model (68) asymptotically approaches to the soft limiter model [36] as ω increases.

To confirm the analysis in Section IV-C that the DL estimator can well approximate the MMSE estimator, we illustrate the squared biases of the LMMSE and the DL estimators versus SNR for channel estimation under nonlinear model (68) with $t_0 = 1$ in Fig. 4(a). The saturation level is fixed as 1.5 and the smoothness factor is set to be 1 as before. The squared biases of the LMMSE and the DL estimators are the bias terms in (42) and (43), respectively, and are computed w.r.t. $x_0 = 0.5$, where x_0 denotes

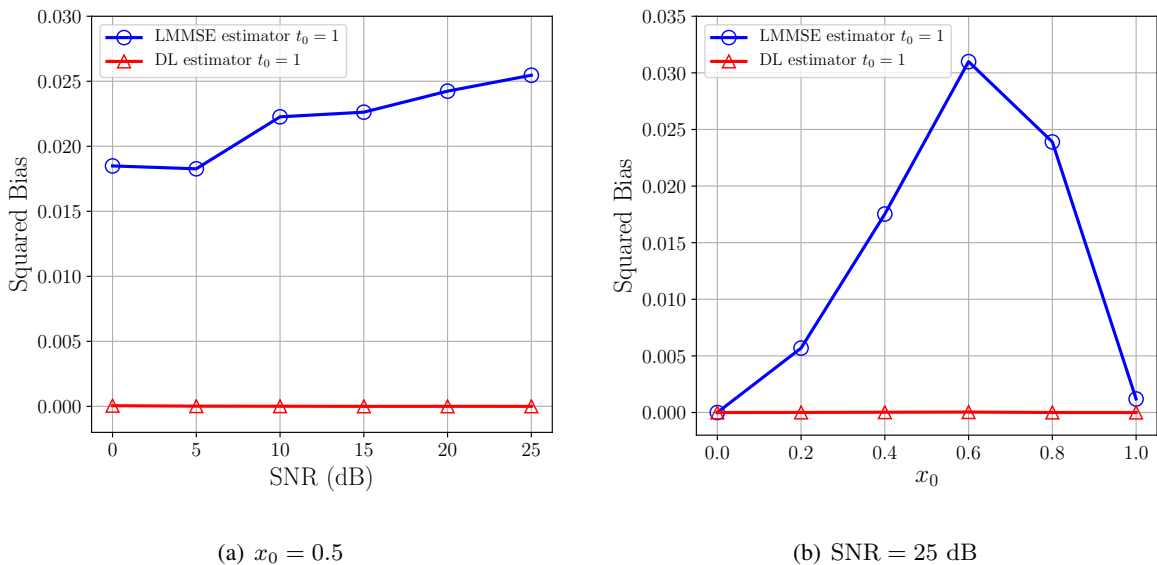


Fig. 4. The squared bias performance of the LMMSE and the DL estimators versus SNR under nonlinear signal model; (b) The squared bias performance of the LMMSE and the DL estimators versus x_0 under nonlinear signal model.

x_0 when $t_0 = 1$. Since no analytic form of \mathbf{h}_{MMSE} for nonlinear model (68) is available, we use Monte Carlo simulation to estimate \mathbf{h}_{MMSE} in Fig 4(a) and the number of trials is set as 2×10^7 . From the figure, the squared biases of the DL estimator are always close to zero across the entire range of SNRs. In comparison, the squared biases of the LMMSE estimator are much higher. Such results verify the analysis in Section IV-C that the DL estimator can well approximate $\hat{\mathbf{h}}_{\text{MMSE}}$ and outperform the LMMSE estimator in nonlinear systems.

Fig. 4(b) illustrates the squared biases of the LMMSE and the DL estimators versus x_0 under nonlinear model (68) with $t_0 = 1$ and SNR = 25 dB. The saturation level and the smoothness factor are the same with that in Fig. 4(a). The squared biases of the LMMSE estimator fluctuates across different input points and are significantly larger than those of the DL estimator. The reason for this fluctuation is that the LMMSE estimator uses a linear function to approximate the nonlinear model (68), and the squared biases at different input points differ dramatically due to the nonlinearity. As shown in Fig. 4(b), the cross points of the LMMSE and the MMSE estimators are close to $x_0 = 0$ and $x_0 = 1$ while the LMMSE estimator departs most farther at $x_0 = 0.6$. On the contrary, the squared biases of the DL estimator are close to zero at different input points. It further verifies the analysis in Section IV-C that the universal approximation of the DL estimator to $\hat{\mathbf{h}}_{\text{MMSE}}$ is applicable to a wide range of inputs.

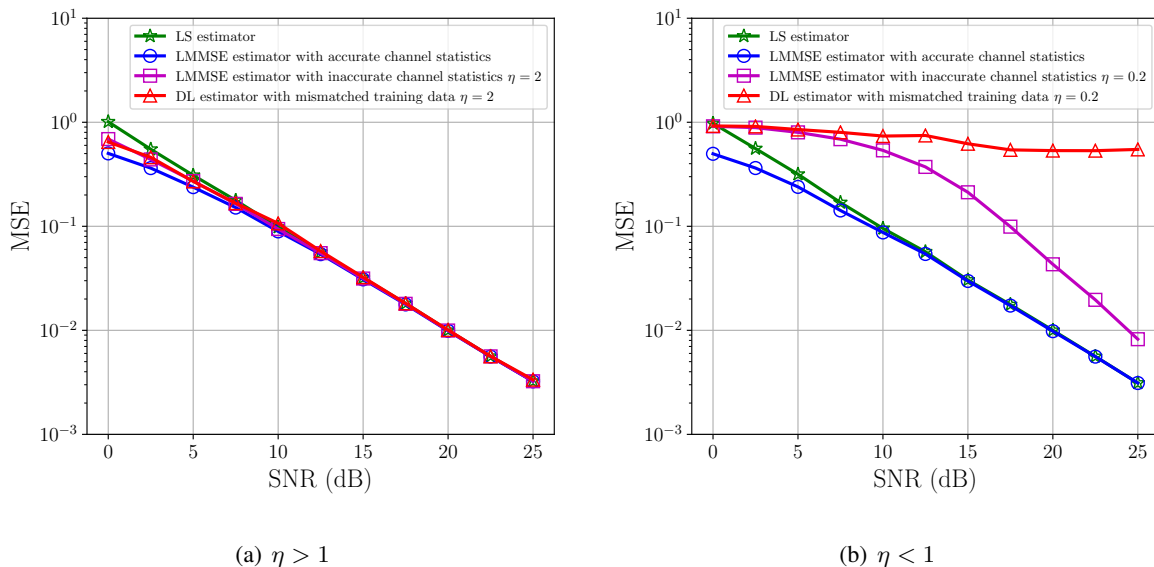


Fig. 5. The MSE performance of the LMMSE and the DL estimators versus SNR when statistics of channel and training data are inaccurate.

C. Robustness to Mismatched Information

We then compare the MSEs of channel estimation using the LMMSE and the DL estimators when statistics of channel and training data are inaccurate in linear systems. Assume that $\mathbf{R}_1 = \sigma_1^2 \mathbf{I}_{t_0}$ and $\mathbf{R}_{\text{er}} = \sigma_{\text{er}}^2 \mathbf{I}_{t_0}$, where σ_1^2 and σ_{er}^2 are the element-wise variances. Moreover, we define the scaling coefficient η as the ratio σ_1^2/σ^2 or $\sigma_{\text{er}}^2/\sigma^2$. The other settings are the same with Section VI-A. When $\eta > 1$, i.e., Case 1 in Section V-B, the performance of the DL estimator is only affected by the inaccuracy of the training data. When $\eta < 1$, i.e., Case 2 in Section V-B, the DL estimator may malfunction and outputs random estimates.

Fig. 5(a) illustrates the MSEs of the LMMSE and the DL estimators versus SNR for channel estimation under linear signal model in (1) with $\eta = 2$ and $t_0 = 1$. The MSEs of the LMMSE estimator with accurate channel statistics and the LS estimator are served as the benchmarks. In Fig. 5(a), both the LMMSE estimator with inaccurate channel statistics and the DL estimator with mismatched training data perform poorer than the LMMSE estimator with accurate channel statistics but still better than the LS estimator. Furthermore, under the same η , the MSEs of the LMMSE with inaccurate statistics and the DL estimator with mismatched training data are overlapped, which confirms the results in (57) and (65). Specifically, in high SNRs, the MSEs of these estimators are almost the same and the errors of channel statistics have little impact on the overall estimation performance.

Fig. 5(b) illustrates the MSEs of the LMMSE and the DL estimators versus SNR for channel estimation

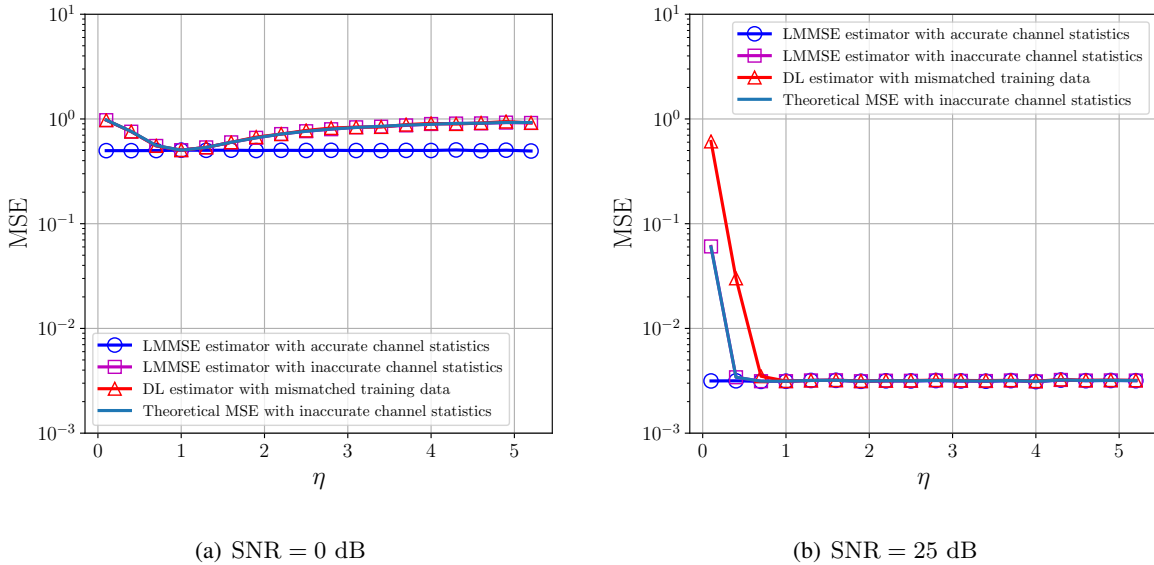


Fig. 6. The MSE performance of the LMMSE and the DL estimators versus η .

under linear signal model in (1) with $\eta = 0.2$ and $t_0 = 1$. When $\eta < 1$, the MSE of the LMMSE estimator with inaccurate channel statistics is significantly larger than those of the LS and LMMSE estimators with accurate channel statistics. The performance of the LMMSE estimator with inaccurate channel statistics degrades more severely than the case in Fig. 5(a) where $\eta > 1$. The performance of the DL estimator is even worse where its MSE is totally random and uncorrelated to the SNR. Such phenomenon verifies the analysis in Section V-B when the variance of training data is lower than that of true channel, i.e., $\eta < 1$. Therefore, the mismatch of training data with the true environment is a serious problem if $\eta < 1$ and should be carefully considered when applying DL methods in wireless communication systems.

Fig. 6 visualizes the MSEs of the LMMSE estimator with inaccurate channel statistics and the DL estimator with mismatched training data versus η for channel estimation under linear signal model (1) when $t_0 = 1$ and SNRs are fixed. The MSE of the LMMSE estimator with accurate channel statistics is used as the benchmark. Since the LMMSE estimator is effective over the whole input space, we adopt the MSE of the LMMSE estimator with inaccurate channel statistics in (57) as the theoretical MSE. In Fig. 6(a), the SNR is fixed as 0 dB. The MSEs of the LMMSE estimator with inaccurate channel statistics and the DL estimator with mismatched training data are overlapped with the theoretical MSE and are slightly higher than the MSE of the LMMSE estimator with accurate channel statistics when $\eta > 1$, which demonstrates that the LMMSE and DL estimators are robust to inaccurate channel statistics. Such a result also verifies the correctness of (57) and (65), as (65) is equivalent to (57) under the same η . When $\eta = 1$, no errors exist and the MSEs of the LMMSE estimator with inaccurate channel statistics and

the DL estimator with mismatched training data are close to that of the LMMSE with accurate channel statistics. When $\eta < 1$, the MSEs of the LMMSE estimator with inaccurate channel statistics and the DL estimator with mismatched training data are larger than that of the LMMSE estimator with accurate channel statistics. Furthermore, both MSEs of the LMMSE estimator with inaccurate channel statistics and the DL estimator with mismatched training data still fit in the theoretical MSE at low SNRs. Such a result demonstrates that the constrained effective input range has little influence on the performance of the DL estimator when SNRs are low. As illustrated in Fig 5(b), the MSE of the LMMSE estimator with inaccurate channel statistics is comparable to that of the DL estimator with mismatched training data at low SNRs. Therefore, the gap between the MSEs of the LMMSE estimator with inaccurate channel statistics and the DL estimator with mismatched training data is not significant in Fig. 6(a).

Fig. 6(b) shows the MSEs of the LMMSE estimator with inaccurate channel statistics and the DL estimator with mismatched training data versus η when $t_0 = 1$ and SNR is fixed as 25 dB. When $\eta \geq 1$, the MSEs of the LMMSE estimator with inaccurate channel statistics and the DL with mismatched training data are almost equal to that of the LMMSE estimator. Therefore, the errors of channel statistics have little influence on the estimation performance of these estimators when $\eta > 1$ and SNR is high. When $\eta < 1$, the MSE of the DL estimator with is significantly larger than that of the LMMSE estimator with inaccurate channel statistics and the theoretical MSE. The reason for this phenomenon is that the estimate of the DL estimator with mismatched training data gets more random as η decreases and is nearly uncorrelated to the SNR when $\eta < 1$, as shown in Fig. 5(b), while the MSE of the LMMSE with inaccurate channel statistics still decreases with the SNR. Therefore, the gap between the MSEs of the LMMSE estimator with inaccurate channel statistics and the DL estimator with mismatched training data becomes much more significant at high SNRs. Such a result verifies the analysis in Section V-B again. Moreover, the MSE of the LMMSE estimator with inaccurate channel statistics matches the theoretical MSE and is slightly higher than the MSE of the LMMSE estimator with accurate channel statistics across the entire range of η , which shows the robustness of the LMMSE estimator to inaccurate channel statistics.

VII. CONCLUSIONS

In this paper, we have made the first attempt on interpreting DL based channel estimation under linear, nonlinear, and inaccurate channel statistics using a multiple antenna system as an example. We have explained that the DL estimator equipped with a ReLU DNN is mathematically equivalent to a set of local linear functions and can attain universal approximation by adjusting the number and the forms of these functions. Then, we have derived a closed-form expression for DL based channel estimation

and compared its estimation performance with the LS and LMMSE estimators under linear and nonlinear systems. We have shown that the target estimator that the DL estimator approaches to under large training samples is the MMSE estimator and the DL estimator can well approximate the MMSE estimator due to universal approximation. Extensive simulation results have confirmed the performance of the DL estimator and showed that the DL estimator is close to the LMMSE estimator under linear systems but significantly outperforms it when the signal model is nonlinear. However, the DL estimator is sensitive to the quality of data, and its performance would significantly degrade if the data in real environments distributes broader than the training data. The benefits of the DL estimator have to weigh against its costs when applied to the channel estimation in real wireless communication systems. Striking a balance between the DL estimation and conventional estimation might be a better choice in the future.

REFERENCES

- [1] T. Wang, C.-K. Wen, H. Wang, F. Gao, T. Jiang, and S. Jin, "Deep learning for wireless physical layer: Opportunities and challenges," *China Commun.*, vol. 14, no. 11, pp. 92–111, Sep. 2017.
- [2] X. Gao, S. Jin, C.-K. Wen, and G. Y. Li, "ComNet: Combination of deep learning and expert knowledge in OFDM receivers," *IEEE Commun. Lett.*, vol. 22, no. 12, pp. 2627–2630, Dec. 2018.
- [3] X. Yang, M. Matthaiou, J. Yang, C.-K. Wen, F. Gao, and S. Jin, "Hardware-constrained millimeter-wave systems for 5G: Challenges, opportunities, and solutions," *IEEE Commun. Mag.*, vol. 57, no. 1, pp. 44–50, Jan. 2019.
- [4] Z. Qin, H. Ye, G. Y. Li, and B.-H. F. Juang, "Deep learning in physical layer communications," *IEEE Wireless Commun.*, vol. 26, no. 2, pp. 93–99, Apr. 2019.
- [5] H. Ye, L. Liang, G. Y. Li, J. Kim, L. Lu, and M. Wu, "Machine learning for vehicular networks: Recent advances and application examples," *IEEE Veh. Technol. Mag.*, vol. 13, no. 2, pp. 94–101, Jun. 2018.
- [6] L. Liang, H. Ye, and G. Y. Li, "Toward intelligent vehicular networks: A machine learning framework," *IEEE Internet Things J.*, vol. 6, no. 1, pp. 124–135, Feb. 2019.
- [7] H. He, C.-K. Wen, S. Jin, and G. Y. Li, "Deep learning-based channel estimation for beamspace mmWave massive MIMO systems," *IEEE Wireless Commun. Lett.*, vol. 7, no. 5, pp. 852–855, Oct. 2018.
- [8] H. Ye, G. Y. Li, and B.-H. Juang, "Power of deep learning for channel estimation and signal detection in OFDM systems," *IEEE Wireless Commun. Lett.*, vol. 7, no. 1, pp. 114–117, Feb. 2018.
- [9] T. Wang, C.-K. Wen, S. Jin, and G. Y. Li, "Deep learning-based CSI feedback approach for time-varying massive MIMO channels," *IEEE Wireless Commun. Lett.*, vol. 8, no. 2, pp. 416–419, Apr. 2019.
- [10] T. O'Shea and J. Hoydis, "An introduction to deep learning for the physical layer," *IEEE Trans. Cogn. Commun. Netw.*, vol. 3, no. 4, pp. 563–575, Dec. 2017.
- [11] H. Ye, G. Y. Li, and B.-H. F. Juang, "Deep reinforcement learning based resource allocation for V2V communications," *IEEE Trans. Veh. Technol.*, vol. 68, no. 4, pp. 3163–3173, Apr. 2019.
- [12] H. Huang, J. Yang, H. Huang, Y. Song, and G. Gui, "Deep learning for super-resolution channel estimation and DOA estimation based massive MIMO system," *IEEE Trans. Veh. Technol.*, vol. 67, no. 9, pp. 8549–8560, Sep. 2018.
- [13] Y. Yang, F. Gao, X. Ma, and S. Zhang, "Deep learning-based channel estimation for doubly selective fading channels," *IEEE Access*, vol. 7, pp. 36 579–36 589, 2019.
- [14] M. Soltani, V. Pourahmadi, A. Mirzaei, and H. Sheikhzadeh, "Deep learning-based channel estimation," *IEEE Commun. Lett.*, vol. 23, no. 4, pp. 652–655, Apr. 2019.

- [15] Y. Yang, F. Gao, G. Y. Li, and M. Jian, "Deep learning based downlink channel prediction for FDD massive MIMO system," *IEEE Commun. Lett.*, 2019.
- [16] S. Dörner, S. Cammerer, J. Hoydis, and S. ten Brink, "Deep learning based communication over the air," *IEEE J. Sel. Topics Signal Process.*, vol. 12, no. 1, pp. 132–143, Feb. 2018.
- [17] H. Ye, G. Y. Li, B.-H. F. Juang, and K. Sivanesan, "Channel agnostic end-to-end learning based communication systems with conditional GAN," in *Proc. 2018 IEEE Globecom Workshops (GC Wkshps)*, Dec. 2018, pp. 1–5.
- [18] C.-K. Wen, W.-T. Shih, and S. Jin, "Deep learning for massive MIMO CSI feedback," *IEEE Wireless Commun. Lett.*, vol. 7, no. 5, pp. 748–751, Mar. 2018.
- [19] G. Cybenko, "Approximation by superpositions of a sigmoidal function," *Math. Contr. Signals Syst.*, vol. 2, no. 4, pp. 303–314, 1989.
- [20] K. Hornik, M. Stinchcombe, and H. White, "Multilayer feedforward networks are universal approximators," *Neural Netw.*, vol. 2, no. 5, pp. 359–366, 1989.
- [21] O. Delalleau and Y. Bengio, "Shallow vs. deep sum-product networks," in *Adv. Neural Inf. Process. Syst. 24 (NeuralIPS)*, Dec. 2011, pp. 666–674.
- [22] M. Bianchini and F. Scarselli, "On the complexity of neural network classifiers: A comparison between shallow and deep architectures," *IEEE Trans. Neural Netw. Learning Syst.*, vol. 25, no. 8, pp. 1553–1565, Aug. 2014.
- [23] M. Telgarsky, "Benefits of depth in neural networks," in *Proc. 29th Ann. Conf. Learning Theo. (COLT)*, Jun. 2016, pp. 1517–1539.
- [24] S. M. Kay, *Fundamentals of Statistical Signal Processing*. Prentice Hall PTR, 1993.
- [25] G. F. Montúfar, R. Pascanu, K. Cho, and Y. Bengio, "On the number of linear regions of deep neural networks," in *Adv. Neural Inf. Process. Syst. 27 (NeuralIPS)*, Dec. 2014, pp. 2924–2932.
- [26] E. Costa, M. Midrio, and S. Pupolin, "Impact of amplifier nonlinearities on OFDM transmission system performance," *IEEE Commun. Lett.*, vol. 3, no. 2, pp. 37–39, Feb. 1999.
- [27] E. Costa and S. Pupolin, "M-QAM-OFDM system performance in the presence of a nonlinear amplifier and phase noise," *IEEE Trans. Commun.*, vol. 50, no. 3, pp. 462–472, Mar. 2002.
- [28] L. Xu, X. Lu, S. Jin, F. Gao, and Y. Zhu, "On the uplink achievable rate of massive MIMO system with low-resolution ADC and RF impairments," *IEEE Commun. Lett.*, vol. 23, no. 3, pp. 502–505, Mar. 2019.
- [29] R. Arora, A. Basu, P. Mianjy, and A. Mukherjee, "Understanding deep neural networks with rectified linear units," in *Int. Conf. Learning Rep. (ICLR)*, 2018.
- [30] W. Mendenhall, R. J. Beaver, and B. M. Beaver, *Introduction to Probability and Statistics*. Cengage Learning, 2012.
- [31] A. Van der Vaart and J. A. Wellner, *Weak Convergence and Empirical Processes*. Springer, New York, 2000.
- [32] S. J. Pan and Q. Yang, "A survey on transfer learning," *IEEE Trans. Knowledge Data Eng.*, vol. 22, no. 10, pp. 1345–1359, Oct. 2009.
- [33] Y. Bar-Shalom, X. R. Li, and T. Kirubarajan, *Estimation with Applications to Tracking and Navigation: Theory Algorithms and Software*. John Wiley & Sons, 2004.
- [34] F. Rusek, D. Persson, B. K. Lau, E. G. Larsson, T. L. Marzetta, O. Edfors, and F. Tufvesson, "Scaling up MIMO: opportunities and challenges with very large arrays," *IEEE Signal Process. Mag.*, vol. 30, no. 1, pp. 40–60, Jan. 2013.
- [35] H. He, S. Jin, C.-K. Wen, F. Gao, G. Y. Li, and Z. Xu, "Model-driven deep learning for physical layer communications," *IEEE Wireless Commun.*, 2019.
- [36] J. Joung, C. K. Ho, K. Adachi, and S. Sun, "A survey on power-amplifier-centric techniques for spectrum-efficient and energy-efficient wireless communications," *IEEE Commun. Surveys Tuts.*, vol. 17, no. 1, pp. 315–333, Firstquarter 2015.